

Groundwater Flow Model of the General Separations Area Using PORFLOW

APPROVED for Release for
Unlimited (Release to Public)

by

GREGORY FLACH

Westinghouse Savannah River Company

Savannah River Site

Aiken, South Carolina 29808

DOE Contract No. **DE-AC09-96SR18500**

This paper was prepared in connection with work done under the above contract number with the U. S. Department of Energy. By acceptance of this paper, the publisher and/or recipient acknowledges the U. S. Government's right to retain a nonexclusive, royalty-free license in and to any copyright covering this paper, along with the right to reproduce and to authorize others to reproduce all or part of the copyrighted paper.

DISCLAIMER

This report was prepared as an account of work sponsored by an agency of the United States Government. Neither the United States Government nor any agency thereof, nor any of their employees, makes any warranty, express or implied, or assumes any legal liability or responsibility for the accuracy, completeness, or usefulness of any information, apparatus, product or process disclosed, or represents that its use would not infringe privately owned rights. Reference herein to any specific commercial product, process or service by trade name, trademark, manufacturer, or otherwise does not necessarily constitute or imply its endorsement, recommendation, or favoring by the United States Government or any agency thereof. The views and opinions of authors expressed herein do not necessarily state or reflect those of the United States Government or any agency thereof.

This report has been reproduced directly from the best available copy.

Available for sale to the public, in paper, from: U.S. Department of Commerce, National Technical Information Service, 5285 Port Royal Road, Springfield, VA 22161

phone: (800) 553-6847

fax: (703) 605-6900

email: orders@ntis.fedworld.gov

online ordering: <http://www.ntis.gov/help/index.asp>

Available electronically at <http://www.osti.gov/bridge>

Available for a processing fee to U.S. Department of Energy and its contractors, in paper, from: U.S. Department of Energy, Office of Scientific and Technical Information, P.O. Box 62, Oak Ridge, TN 37831-0062

phone: (865) 576-8401

fax: (865) 576-5728

email: reports@adonis.osti.gov

WSRC-TR-2004-00106
Revision 0

KEY WORDS: PORFLOW code
FACT code
Groundwater flow

**GROUNDWATER FLOW MODEL OF THE
GENERAL SEPARATIONS AREA USING PORFLOW (U)**

JULY 15, 2004

**PREPARED BY:
Gregory P. Flach^a**

APPROVED for Release for
Unlimited (Release to Public)

^aWestinghouse Savannah River Company LLC



Westinghouse Savannah River Company LLC
Savannah River Site
Aiken, SC 29808

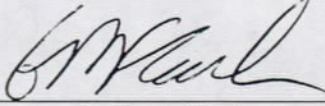
Prepared for the U.S. Department of Energy under Contract No. DE-AC09-96SR18500

DISCLAIMER

This report was prepared by Westinghouse Savannah River Company LLC for the United States Department of Energy under Contract No. DE-AC09-96SR18500 and is an account of work performed under that contract. Reference herein to any specific commercial product, process, or service by trademark, name, manufacturer, or otherwise does not necessarily constitute or imply endorsement, recommendation, or favoring of same by Westinghouse Savannah River Company LLC or by the United States Government or any agency thereof.

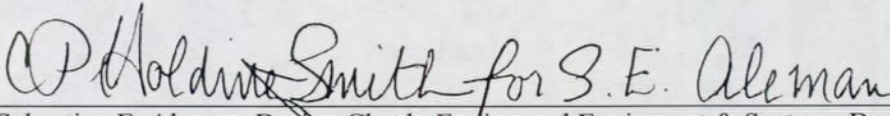
REVIEWS AND APPROVALS

Author

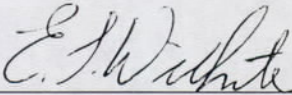
7/29/04

Gregory P. Flach, Environmental Sciences & Technology Department Date

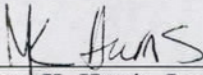
Reviews/Approvals

7/29/04

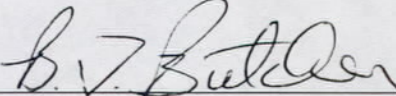
Sebastian E. Aleman, Design Check, Engineered Equipment & Systems Department Date

7/29/04

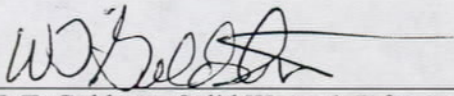
Elmer L. Wilhite, Design Check, Waste Processing Technology Department Date

7/29/04

Mary K. Harris, Level 4, Environmental Sciences & Technology Department Date

7/29/04

Byron T. Butcher, Level 4, Waste Disposal and Environmental Development Date

7/29/04

W. T. Goldston, Solid Waste & Infrastructure Date

THIS PAGE INTENTIONALLY LEFT BLANK

TABLE OF CONTENTS

| | |
|--|-----|
| 1.0 INTRODUCTION | 1 |
| 2.0 MIGRATION FROM FACT TO PORFLOW | 3 |
| 2.1 Computational Mesh | 3 |
| 2.2 Boundary Conditions | 3 |
| 2.3 Material Properties | 5 |
| 2.4 Implementation of Recharge/Drain BC | 5 |
| 2.5 Model Recalibration | 6 |
| 3.0 STEADY-STATE GROUNDWATER FLOW SIMULATION | 14 |
| 3.1 Hydraulic Head | 14 |
| 3.2 Groundwater Flows | 14 |
| 4.0 VERIFICATION AND VALIDATION | 21 |
| 4.1 Conservation of Mass | 21 |
| 4.2 Darcy's Law | 22 |
| 4.3 Stratigraphy | 23 |
| 4.4 Hydraulic Conductivity | 23 |
| 4.5 Hydraulic Head | 23 |
| 4.6 Recharge and Stream Baseflows | 24 |
| 4.7 Particle Tracking and Solute Transport | 25 |
| 4.8 Summary Assessment | 25 |
| 5.0 CONCLUSIONS AND RECOMMENDATIONS | 30 |
| 6.0 REFERENCES | 32 |
| APPENDIX A - QUALITATIVE COMPARISON OF GSA/PORFLOW HORIZONTAL CONDUCTIVITY FIELD TO CHARACTERIZATION DATA | A-1 |

LIST OF FIGURES

| | | |
|------------|---|----|
| Figure 2-1 | Cross-sectional view of computational mesh for (a) FACT, and (b) PORFLOW | 8 |
| Figure 2-2 | Plan view of GSA/FACT and GSA/PORFLOW computational meshes | 9 |
| Figure 2-3 | Perspective view of GSA/PORFLOW computational mesh | 9 |
| Figure 2-4 | Combined recharge and drain boundary condition used in GSA/FACT and GSA/PORFLOW models | 10 |
| Figure 2-5 | Boundary conditions applied to GSA/PORFLOW computational mesh | 11 |
| Figure 2-6 | Cross-sectional view of horizontal hydraulic conductivity field for (a) FACT, and (b) PORFLOW | 12 |
| Figure 2-7 | Pseudo soil characteristic curves | 13 |
| Figure 2-8 | Example velocity field showing predominantly downward flow in the vadose zone; vectors are fixed length showing flow direction only | 13 |
| Figure 3-1 | Simulated hydraulic head over the top surface of the GSA/PORFLOW mesh .. | 16 |
| Figure 3-2 | Simulated hydraulic head in GSA/PORFLOW model at cross-section through E Area (I=50) | 16 |
| Figure 3-3 | GSA/PORFLOW results for the UTR upper aquifer zone: (a) vertically-averaged head, and (b) residuals between computed and measured heads | 17 |
| Figure 3-4 | GSA/PORFLOW results for the UTR lower aquifer zone: (a) vertically-averaged head, and (b) residuals between computed and measured heads | 18 |
| Figure 3-5 | GSA/PORFLOW results for the Gordon aquifer unit: (a) vertically-averaged head, and (b) residuals between computed and measured heads | 19 |
| Figure 3-6 | Simulated seepage areas in GSA/PORFLOW model compared to available seepage survey data | 20 |
| Figure 3-7 | Simulated surface flux in GSA/PORFLOW model with positive values indicating groundwater discharge (ft^3/d) | 20 |
| Figure 4-1 | GSA/PORFLOW representation of the top of the Meyers Branch confining system (Crouch Branch confining unit) | 26 |
| Figure 4-2 | GSA/PORFLOW representation of the top of the Gordon aquifer unit | 26 |
| Figure 4-3 | GSA/PORFLOW representation of the top of the Gordon confining unit | 27 |
| Figure 4-4 | GSA/PORFLOW representation of the top of the UTR lower aquifer zone | 27 |
| Figure 4-5 | GSA/PORFLOW representation of the top of the UTR tan clay confining zone | 28 |
| Figure 4-6 | Particle tracking simulation with 5 year markers for (a) GSA/FACT and (b) GSA/PORFLOW | 29 |

LIST OF TABLES

| | | |
|------------------|---|-----------|
| Table 3-1 | Summary statistics for hydraulic head residuals | 14 |
| Table 3-2 | Comparison of measured and simulated stream baseflow | 15 |
| Table 4-1 | Global mass balance for GSA/PORFLOW model | 21 |
| Table 4-2 | Summary of cell-by-cell mass balance for GSA/PORFLOW model | 22 |
| Table 4-3 | Summary of testing to confirm Darcy's law is satisfied at saturated internal cell faces..... | 23 |
| Table 4-4 | Summary statistics for hydraulic head residuals in GSA/FACT | 24 |
| Table 4-5 | Comparison of measured and simulated stream baseflow in GSA/FACT | 24 |
| Table 4-6 | Tritium transport simulations for various LAW vault footprints following Flach and Millings (2003) | 25 |

LIST OF ACRONYMS AND ABBREVIATIONS

ACRONYMS

| | |
|------|---|
| ACRi | Analytic & Computational Research, Incorporated |
| BC | boundary condition |
| FACT | Subsurface Flow and Contaminant Transport code |
| GSA | General Separations Area |
| LAW | Low Activity Waste |
| LLC | Limited Liability Company |
| PA | Performance Assessment |
| QA | Quality Assurance |
| SRS | Savannah River Site |
| TCCZ | Tan Clay Confining Zone |
| UTR | Upper Three Runs |
| V&V | verification and validation |

ABBREVIATIONS

| | |
|-----|------------------------|
| d | day |
| ft | feet |
| in | inches |
| K | hydraulic conductivity |
| msl | mean sea level |
| yr | year |

1.0 INTRODUCTION

The E Area PA (McDowell-Boyer et al. 2000) includes a steady-state simulation of groundwater flow in the General Separations Area as a prerequisite for saturated zone contaminant transport analyses. The groundwater flow simulations are based on the FACT code (Hamm and Aleman 2000). The FACT-based GSA model was selected during preparation of the original PA to take advantage of an existing model developed for environmental restoration applications at the SRS (Flach and Harris 1997, 1999; Flach 1999). The existing GSA/FACT model was then slightly modified for PA use, as described in the PA document. FACT is a finite-element code utilizing deformed brick elements. Material properties are defined at element centers, and state variables such as hydraulic head are located at element vertices. The PORFLOW code (Analytic & Computational Research, Inc. 2000) was selected for performing saturated zone transport simulations of source zone radionuclides and their progeny. PORFLOW utilizes control volume discretization and the nodal point integration method, with all properties and state variables being defined at the center of an interior grid cell.

The groundwater flow calculation includes translating the Darcy velocity field computed by FACT into a form compatible for input to PORFLOW. The FACT velocity field is defined at element vertices, whereas PORFLOW requires flux across cell faces. For the present PA, PORFLOW cell face flux is computed in a two-step process. An initial face flux is computed from FACT as an average of the normal components of Darcy velocity at the four corners. The derived flux field approximately conserves mass, but not rigorously. Thus, the flux field is subsequently perturbed to force rigorous mass conservation on a cell-by-cell basis. The undocumented process used is non-unique and can introduce significant artifacts into the final flux field.

Another issue with using both FACT and PORFLOW for saturated modeling is the different mesh numbering systems used by the two codes. Both codes share the identical mesh, but the (I,J,K) element/cell numbering indices differ by one. The different numbering scheme has led to errors in defining source zones.

The GSA groundwater model will soon be updated to reflect characterization and monitoring data acquired since the original development to support the Saltstone PA revision. The decision was made to also migrate from FACT to PORFLOW for groundwater flow simulations. The motivation is to consolidate all flow and transport analyses to a single software product, and avoid technical issues related to code differences, such as those discussed above.

This report describes how the FACT-based GSA flow model described in the PA has been converted to PORFLOW 5.95.0 (03 MAR 2004), the latest version available to Westinghouse Savannah River Company LLC under license from ACRI. Verification and validation testing pertaining to the new GSA/PORFLOW groundwater flow model following the PORFLOW Software QA Plan (Collard 2002) is also described.

THIS PAGE INTENTIONALLY LEFT BLANK

2.0 MIGRATION FROM FACT TO PORFLOW

In migrating the existing GSA/FACT groundwater flow model to PORFLOW, the main objective was to effect only a change of simulation software. To this end, the original characterization and monitoring datasets, pre-processing algorithms, and model calibration strategies were retained largely intact. Nevertheless, differences between the two codes lead to notable exceptions which are described in the sections below. Flach and Harris (1999), Flach (1999) and the PA (McDowell-Boyer et al. 2000) provide additional information about the baseline GSA/FACT model.

2.1 Computational Mesh

The computational mesh used with FACT conforms to the ground surface as shown in Figure 2-1a. Note that model layers are not truncated by the ground surface, but rather become thin and follow the ground surface beyond outcrops. The resulting mesh contains significantly distorted grid cells. FACT is capable of accurately representing the velocity field, despite element distortion, when the Gaussian quadrature option is used (Hamm and Aleman 2000). However, distorted grid cells are undesirable for PORFLOW, and thin grid cells can lead to severe time step constraints due to high cell Courant numbers when simulating contaminant transport.

Therefore, the logic for constructing the computational mesh was modified for PORFLOW to truncate mesh layers at the ground surface. Also, the mesh layers above the tan clay confining zone are non-uniformly distributed between the TCCZ and an elevation of 325 ft msl, rather than uniformly distributed between the TCCZ and ground surface in GSA/FACT. A cross-section of the GSA/PORFLOW mesh, comparable to Figure 2-1a, is shown in Figure 2-1b. Note that the layering below the tan clay confining zone is essentially the same between the two models. In E Area, the water table occurs just above the tan clay confining zone. To approximately preserve the vertical mesh resolution of the GSA/FACT model in the saturated zone between the water table and tan clay, a non-uniform distribution of layers is used in the PORFLOW grid.

The meshes are identical in plan view, with a nominal spacing of 200 ft square (Figure 2-2). Figure 2-3 provides a perspective view of the entire PORFLOW mesh looking toward the northeast in the SRS coordinate system.

2.2 Boundary Conditions

Four types of boundary conditions are used in the GSA/FACT model as depicted in Figure 2-2: prescribed head, general head, combined recharge and drain, and no flow. From a physical perspective, the same boundary conditions are effectively applied in the GSA/PORFLOW model, with a few exceptions:

1. The maximum recharge rate has been increased from 18 in/yr in the GSA/FACT model to 19 in/yr in the GSA/PORFLOW model, for reasons discussed further in section 2.5 on model recalibration.
2. Recharge/drain BCs are applied over the entire top of the mesh in the GSA/FACT model, including areas also receiving general head BCs. Implementation of two BCs at the same location was an apparent oversight. For the GSA/PORFLOW model, only one BC is allowed at a cell face.
3. The independent variable in the recharge/drain BC is defined to be pressure head ($\psi = p / \rho g = h - z$) in FACT. For the GSA/PORFLOW model, the independent variable is chosen as the product of pressure head and a normalized vertical conductivity at the face,

$$\psi' = \psi \frac{K_v}{K_{ref}} \quad (\text{Eq. 2-1})$$

where K_{ref} is set to 1 ft/d. The functional form of the recharge/drain BC is shown in Figure 2-4 for reference. The modification was made to mitigate numerical convergence issues described in section 2.4, and has little effect on the hydraulic head computed at the boundary face from a physical perspective.

4. Low permeability caps are represented in the GSA/FACT model by setting the conductivity in the uppermost grid layer to a very low value. In the GSA/PORFLOW model, caps are ignored as being unimportant to regional groundwater flow. Thus, material properties just beneath the surface are unaltered and the recharge rate is the same as adjacent areas (Figure 2-4). This modification also alleviates numerical difficulties caused by the presence of a very low permeability surface elements.
5. The general head BC applied to an area described as the "H-area recharge polygon" in Flach and Harris (1999, Figure 18) has been omitted, for reasons discussed in section 2.5 on model recalibration.

Although the boundary conditions are physically very similar between the two models, implementation differs somewhat to accommodate mesh and code differences. In FACT boundary conditions are applied to element vertices, whereas in PORFLOW boundary conditions are applied to cell faces. FACT boundary conditions are translated into PORFLOW boundary conditions using the following logic:

1. Prescribed head boundary conditions defined at boundary cell vertices in the GSA/FACT model are first identified. Boundary faces having 3 or more prescribed head boundary conditions at corners in GSA/FACT receive a prescribed head BC in the GSA/PORFLOW model. The value prescribed on the face is the average of the head values prescribed at vertices. Boundary faces of any orientation (x^- , x^+ , y^- , y^+ , z^- , z^+) are eligible to receive a prescribed head BC.
2. General head boundary conditions are applied in a similar manner, except that only horizontal faces (z^- or z^+) are considered and any existing prescribed head BC takes precedence over a general head BC.
3. Recharge/drain boundary conditions are applied in a similar manner, except that only ground surface faces (z^+ orientation) are eligible and the preceding 2 BCs take precedence. The PORFLOW code does not have an explicit recharge/drain BC option. However, the concept can be implemented using the prescribed flux BC, with flux being set to a certain function of pressure head at the boundary face. Further information is provided in section 2.4.
4. No flow boundary conditions are applied to all remaining boundary faces.

Figure 2-5 illustrates some of the boundary conditions resulting from the above logic.

The greatest difference in boundary condition implementation occurs at the top of each model. In the GSA/FACT model, the top of the mesh smoothly conforms to the ground surface (Figure 2-1a) and each element vertex receives a recharge/drain boundary condition. In the GSA/PORFLOW model, layers crop out at the ground surface producing a stair-step effect (Figure 2-1b). The horizontal z^+ faces receive a recharge/drain or general head BC, and all vertical faces receive a no flow boundary condition (Figure 2-5).

2.3 Material Properties

The algorithm for defining the initial PORFLOW model hydraulic conductivity field is unaltered from that used previously for FACT. However, the three-dimensional K fields for the two models differ due to differences in the grids used (Figure 2-1), and how the respective numerical algorithms use cell properties. In the GSA/PORFLOW, geometric averaging of properties at cell faces was chosen. Differences in the initial K field occur primarily in the volume above the tan clay confining zone. The initial K field in both models was subsequently modified during model calibration to field data. These modifications differ somewhat between FACT and PORFLOW, as discussed in section 2.5, and introduce further differences in the final K fields. Figure 2-6 shows a typical cross-section through the final K field in both models. The fields are similar, but clearly not identical. Additional information about the calibrated GSA/PORFLOW K fields is provided in section 3.0 on model results.

Although the primary focus of the GSA/PORFLOW model is saturated flow beneath the water table, the vadose zone is included in the mesh. Therefore, soil characteristic curves are needed to simulate flow in unsaturated zones. A common practice in this circumstance is to specify "pseudo-soil" characteristic curves that exhibit less non-linearity than actual soil curves. The main function of the vadose zone becomes transfer of water from the ground surface to the water table under steady conditions. Saturations and pressure heads computed in the vadose zone should be largely ignored. The pseudo-soil functions adopted for the GSA/PORFLOW model are depicted in Figure 2-7, and differ somewhat from the GSA/FACT model. The primary modification was to reduce the thickness of the simulated capillary fringe to increase the downward component of vadose zone flows near the water table.

A single set of soil characteristic curves is used in GSA/PORFLOW irrespective of actual soil type. For consistency and to avoid significant lateral flows in unsaturated zones, the saturated hydraulic conductivity field was made uniform in unsaturated zones. Specifically, horizontal and vertical conductivities of cells with a computed saturation less than 90% are set to 0.1 ft/d. The latter value was somewhat arbitrarily chosen to represent average conditions. The homogeneous and isotropic nature of the K field ensures that moisture movement in the vadose zone is vertically downward for practical purposes. The action produces a similar effect to setting the "pk_{rz}" parameter to 1.0 in the FACT code. Figure 2-8 shows simulated velocity at the same cross-section through the GSA/PORFLOW mesh as depicted in earlier figures. Note that above the computed water table, the vectors are predominantly downward, as desired.

Prior to setting K to 0.1 ft/d, significant lateral flows were observed above the water table. This was believed to be an artifact of anisotropy in the K field for saturated conditions, coupled with a homogeneous relative permeability. Anisotropy in the saturated K field was present at the mesh scale (cell horizontal K \gg vertical K), and at larger scales due to a heterogeneous conductivity field that represented strata. The same degree of anisotropy was thus present in the unsaturated K field because the relative permeability curve was identical throughout the mesh. A slight horizontal head gradient produced large horizontal flows. In reality, relative permeability fields for coarse and fine-grained sediments tend to crossover at a certain water saturation. At a sufficiently low saturation, a coarse-grained material will have lower permeability than a fine-grained. This counteracts the anisotropy present under saturated conditions and leads to largely vertical flow in response to a largely vertical gradient.

2.4 Implementation of Recharge/Drain BC

In FACT, the recharge/drain concept is implemented as a kind of mixed (Cauchy) boundary condition, similar to the "general head" and "drain" BCs. Non-linear equations representing the recharge/drain BC at various nodes are included in the overall system of equations being solved

at each numerical step. Thus, pressure heads at a recharge/drain BC nodes are solved implicitly with other unknown (e.g. interior) pressures.

PORFLOW includes a mixed boundary condition equivalent to the "general head" BC in FACT, but does not offer a recharge/drain BC option. An initial attempt to implement the recharge/drain concept using a prescribed flux BC, with flux defined to be the function of pressure head shown in Figure 2-4, proved numerically unstable. PORFLOW performs the boundary pressure head and flux calculations in between time steps in an explicit manner. Apparently the recharge/drain equation was not sufficiently coupled to the system of other equations being solved simultaneously.

To mitigate numerical instability, an under-relaxation scheme was implemented. The basic idea of under-relaxation is to dampen the perturbations in boundary pressure that would otherwise occur. Although the calculation is still explicit, under-relaxation produces adequate numerical stability. The precise calculation sequence used in the GSA/PORFLOW model is

1. At the beginning of step n , set the boundary flux at a recharge/drain BC based on the pressure head from the previous step (cf. Figure 2-4)

$$q_n = q(\psi'_{n-1}) \quad (\text{Eq. 2-2})$$

2. Solve the non-linear system of equations for pressure head at the center of the grid cell with a recharge/drain BC, ψ_n^I .
3. Compute a preliminary new boundary pressure head, $\tilde{\psi}_n$, using Darcy's law

$$q_n = -K_v \frac{\tilde{\psi}_n - \psi_n^I}{z - z^I} \quad (\text{Eq. 2-3})$$

4. Set the final boundary pressure using under-relaxation, where $0 < \omega < 1$

$$\psi_n = \psi_{n-1} + \omega(\tilde{\psi}_n - \psi_{n-1}) \quad (\text{Eq. 2-4})$$

5. Compute the pressure head and conductivity product

$$\psi'_n = \psi_n \frac{K_v}{K_{ref}} \quad (\text{Eq. 2-5})$$

The under-relaxation parameter should be set to roughly 0.5 when the flow field is undergoing a transient, and then be reduced as steady-state conditions are approached. Under the latter conditions, values in the range $0.01 < \omega < 0.1$ are effective at dampening numerical instabilities.

2.5 Model Recalibration

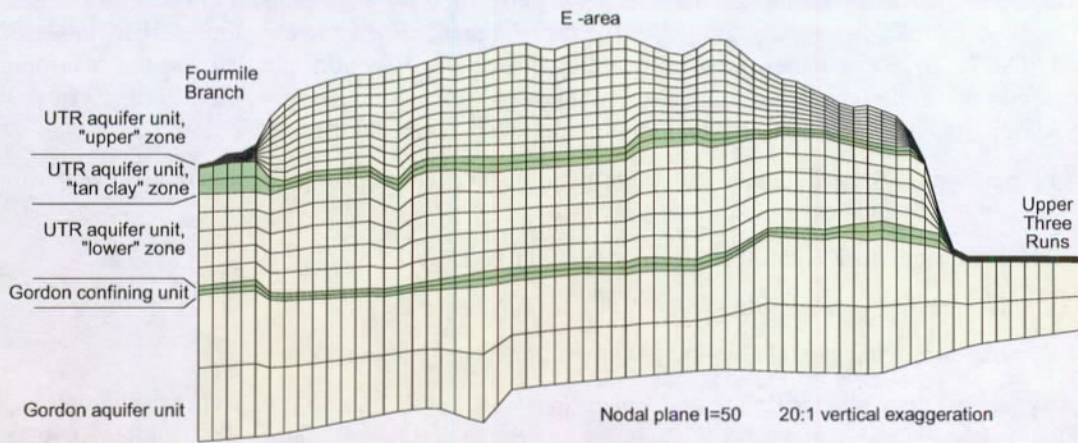
During calibration of the original GSA/FACT model, recharge was increased over H-area to produce simulated heads observed in the field (Flach and Harris, 1999, p. 21). Increased recharge was based on speculation that process water leaks produced an artificial source of recharge in H-area. Presently, high well water levels are believed to be the result of a low permeability confining zone beneath part of H-area, and perhaps lower horizontal conductivity. Therefore, supplemental recharge in H-area was omitted in the GSA/PORFLOW model. Instead, conductivities around H-area were adjusted downward during recalibration to match measured well levels.

After preliminary adjustments to the GSA/PORFLOW conductivity fields to match hydraulic head targets, particle tracking simulations were performed for both models in order to compare groundwater travel times. GSA/PORFLOW travel times were generally longer than those for GSA/FACT. To better match travel times and subsequent transport simulations, the maximum recharge rate in the recharge/drain BC was increased from 18 in/yr in GSA/FACT to 19 in/yr in GSA/PORFLOW. As an additional although minor step, capped areas were ignored.

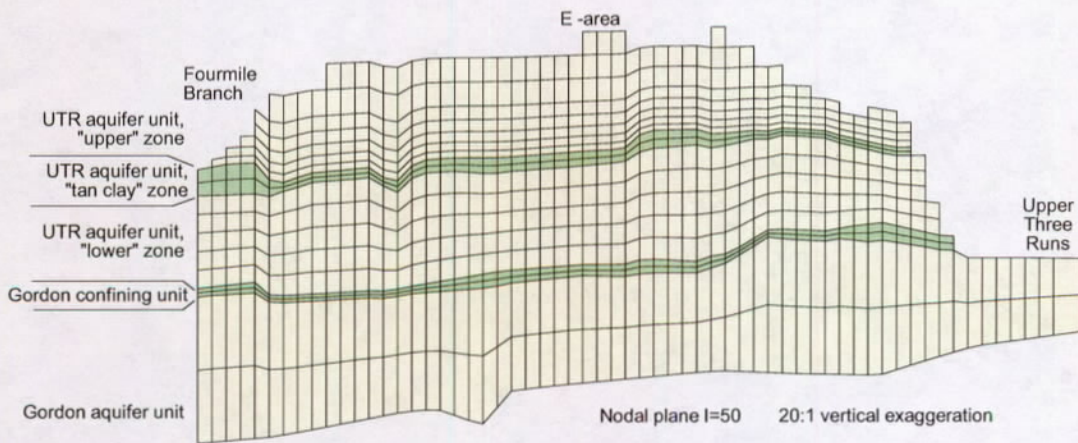
Relative to the GSA/FACT model, the modifications needed to GSA/PORFLOW achieve similar calibration results included

1. Increasing horizontal K in the upper aquifer zone by 25%
2. Decreasing vertical K in the tan clay confining zone by 50%
3. Increasing horizontal K in the lower aquifer zone by about 35%.

A few more minor changes were also made (see the `./MatProp/Cal.dat` files for each model for a precise comparison). Changes to the K field were larger than anticipated and probably reflect geometric averaging at cell faces in PORFLOW versus the corresponding logic used in FACT.



(a)



(b)

Figure 2-1. Cross-sectional view of computational mesh for (a) FACT, and (b) PORFLOW.

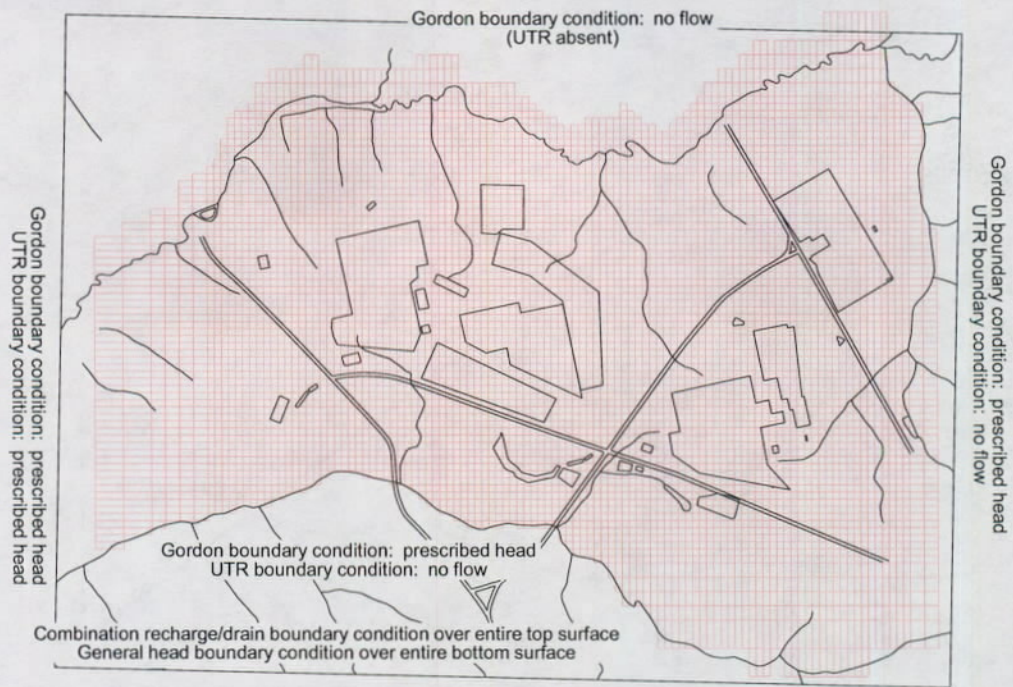


Figure 2-2. Plan view of GSA/FACT and GSA/PORFLOW computational meshes.

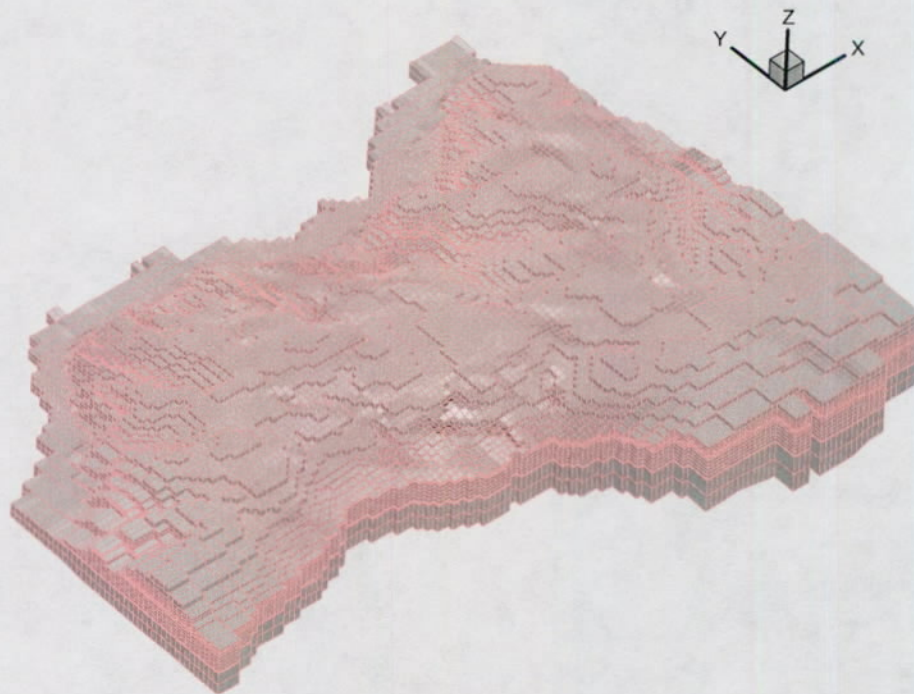


Figure 2-3. Perspective view of GSA/PORFLOW computational mesh.

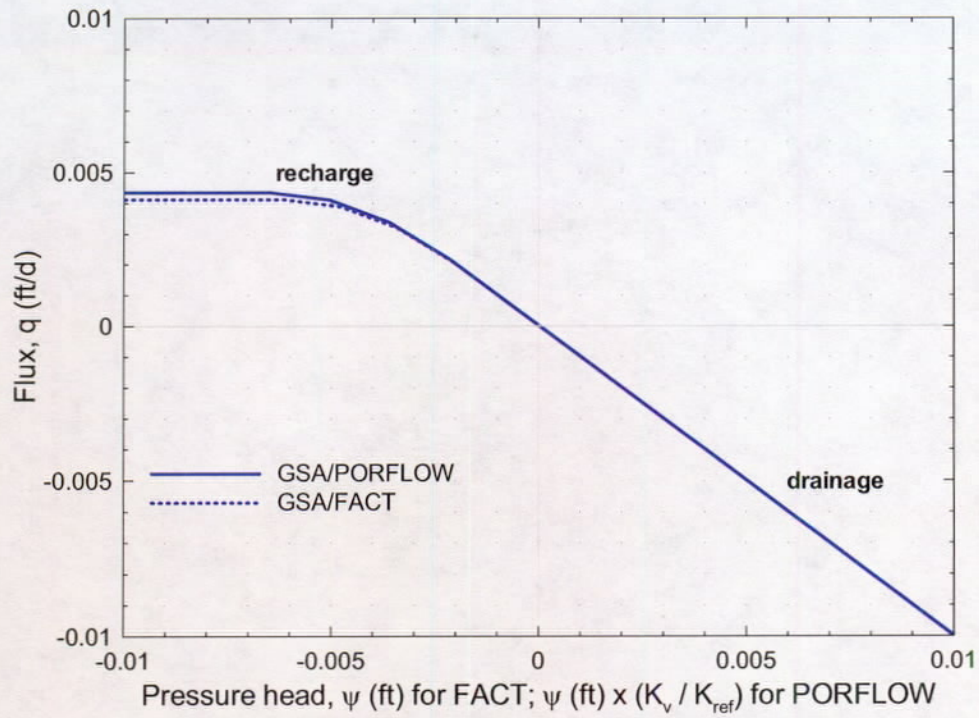
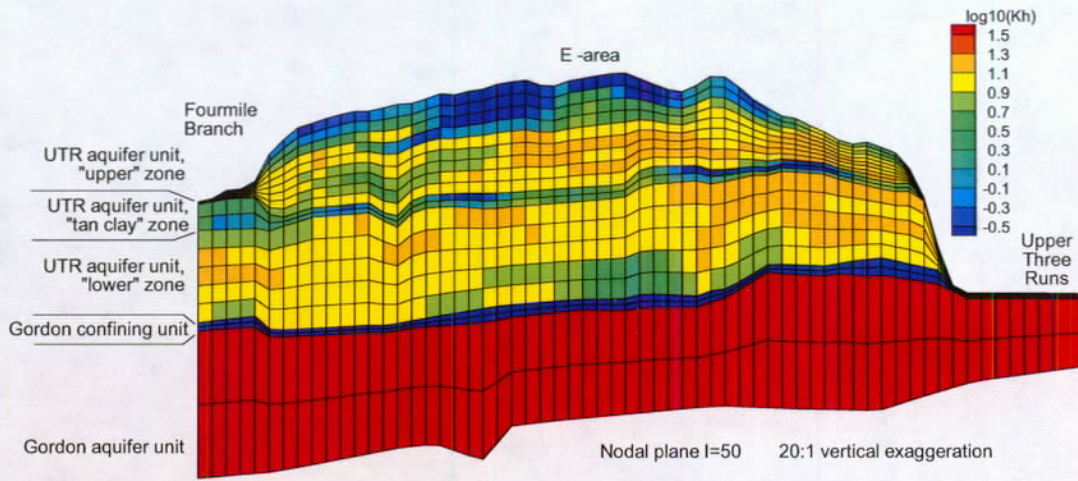


Figure 2-4. Combined recharge and drain boundary condition used in GSA/FACT and GSA/PORFLOW models.

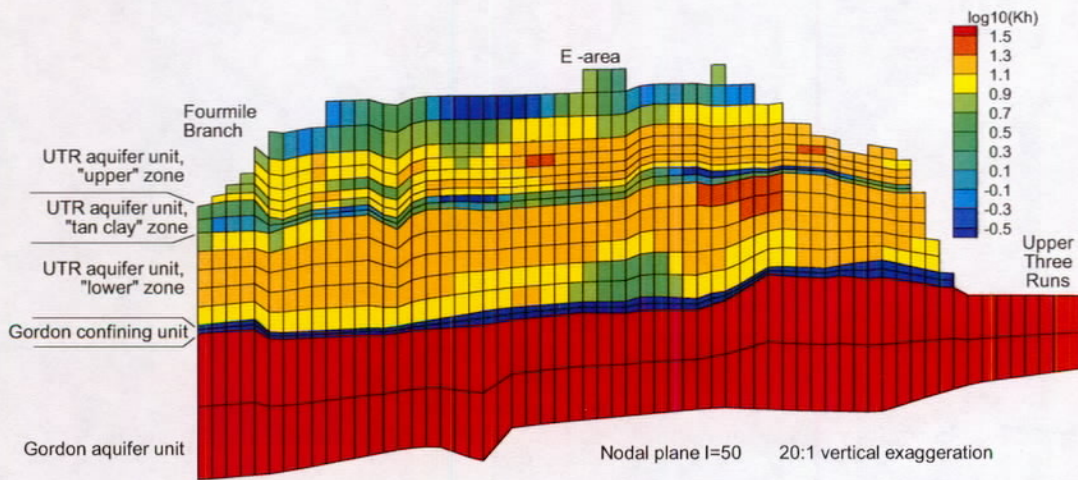


Cross-hatching key
blue = prescribed head
red = general head
green = recharge/drain
yellow = no flow

Figure 2-5. Boundary conditions applied to GSA/PORFLOW computational mesh.



(a)



(b)

Figure 2-6. Cross-sectional view of horizontal hydraulic conductivity field for (a) FACT, and (b) PORFLOW.

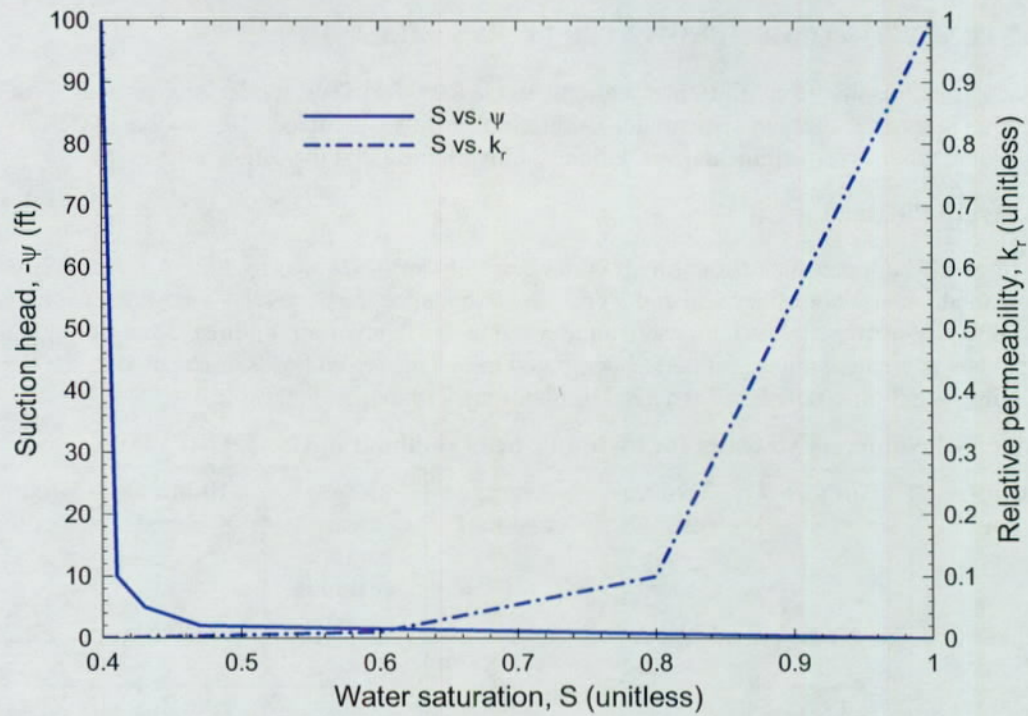


Figure 2-7. Pseudo soil characteristic curves.

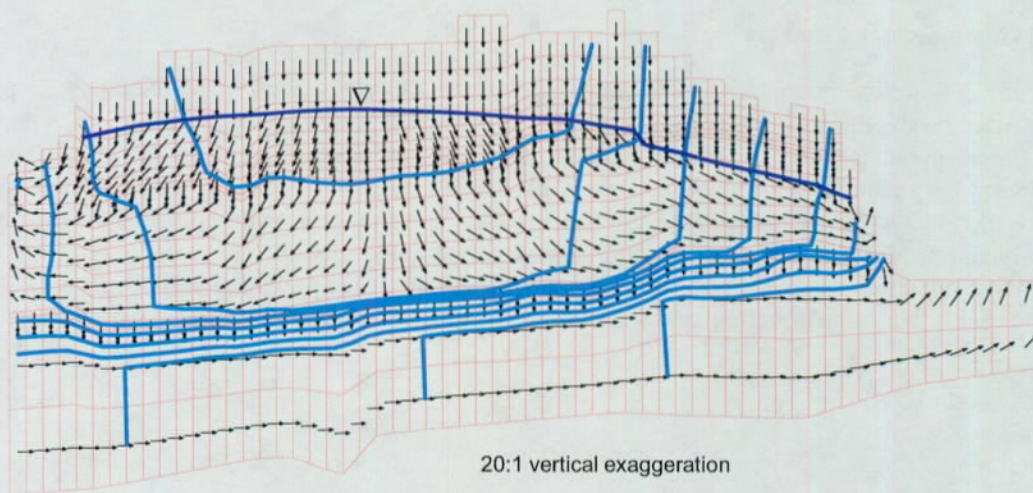


Figure 2-8. Example velocity field showing predominantly downward flow in the vadose zone; vectors are fixed length showing flow direction only.

3.0 STEADY-STATE GROUNDWATER FLOW SIMULATION

Steady-state results from the final calibrated GSA/PORFLOW model are presented in this section. Summary measures of model calibration are also included. Discussion of results and additional model verification and validation testing are provided in section 4.0.

3.1 Hydraulic Head

Portions of the three-dimensional hydraulic head field are shown in Figures 3-1 and 3-2, which show the top surface of the mesh and a cross-sectional slice, respectively. Two-dimensional plots of vertically-averaged head in each aquifer zone are shown in Figures 3-3a through 3-5a. Residuals at well locations, defined as computed minus measured heads, are shown in the Figures 3-3b through 3-5b. Statistics of the head residuals are summarized in Table 3-1.

Table 3-1. Summary statistics for hydraulic head residuals in GSA/PORFLOW.

| Aquifer zone | Number | Median residual (ft) | Average residual (ft) | Root-mean-square residual (ft) | Minimum residual (ft) | Maximum residual (ft) |
|--------------|--------|-------------------------|--------------------------|-----------------------------------|--------------------------|--------------------------|
| Gordon | 79 | -0.0 | -0.5 | 1.7 | -4.7 | 2.5 |
| lower UTR | 173 | +0.8 | +0.6 | 4.6 | -9.4 | 27.0 |
| upper UTR | 386 | -0.1 | -0.5 | 3.4 | -15.2 | 10.0 |

3.2 Groundwater Flows

Figure 3-6 defines seepage faces simulated by the GSA/PORFLOW model. The seepage predicted by the model is the border between recharge (red) and discharge (blue) areas. A survey of the seepage in the early 1990's is shown in the figure for comparison. The flux of water entering the model at the ground surface is shown in Figure 3-7. Groundwater discharge areas correspond to positive flux values. Figures 3-6 and 3-7 are similar with the former indicating only the direction of water flow and the latter showing magnitude as well. The average recharge rate for the model, defined as top surface inflow divided by total area including seepage faces, is 14.7 in/yr. Table 3-2 compares simulated and measured values of recharge and stream baseflow.

Table 3-2. Comparison of measured and simulated stream baseflow in GSA/PORFLOW.

| Stream | Estimated baseflow contribution from GSA (ft³/s) | Simulated baseflow contribution from GSA (ft³/s) |
|---|--|--|
| Upper Three Runs and tributaries excluding McQueen Branch | 18.2 | 11.4 |
| Fourmile Branch and tributaries | 2.6 | 3.8 |
| McQueen Branch | 1.5 | 2.4 |
| Crouch Branch | 1.8 | 1.7 |

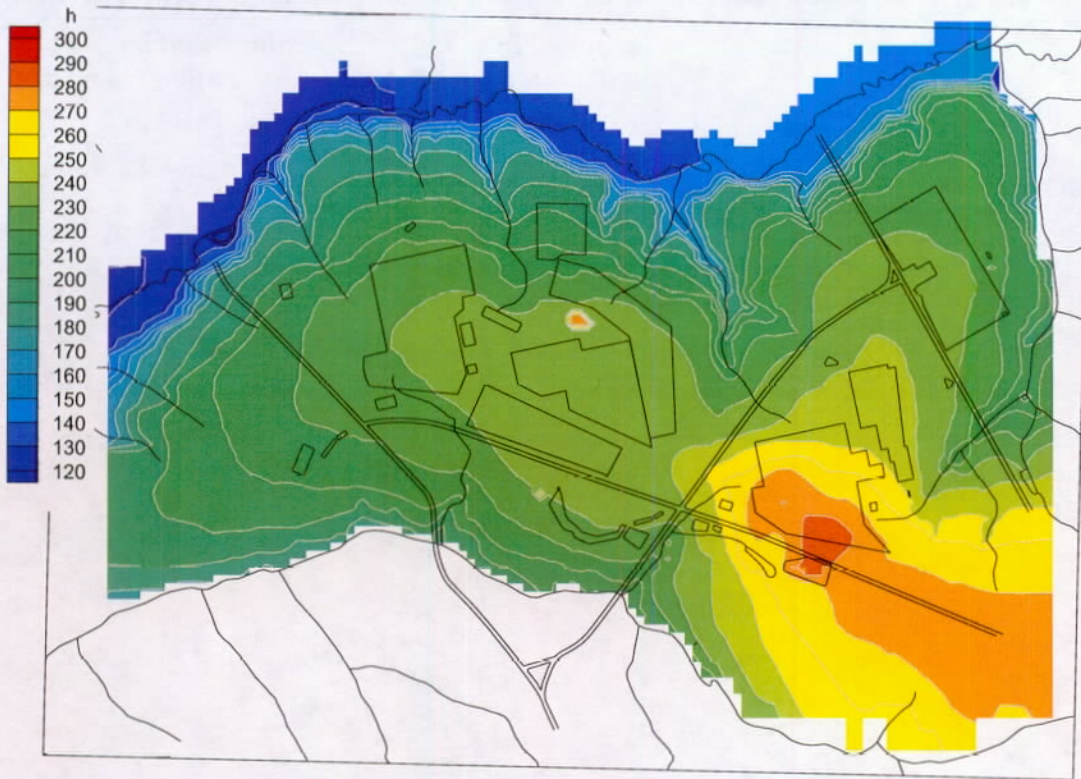


Figure 3-1. Simulated hydraulic head over the top surface of the GSA/PORFLOW mesh.

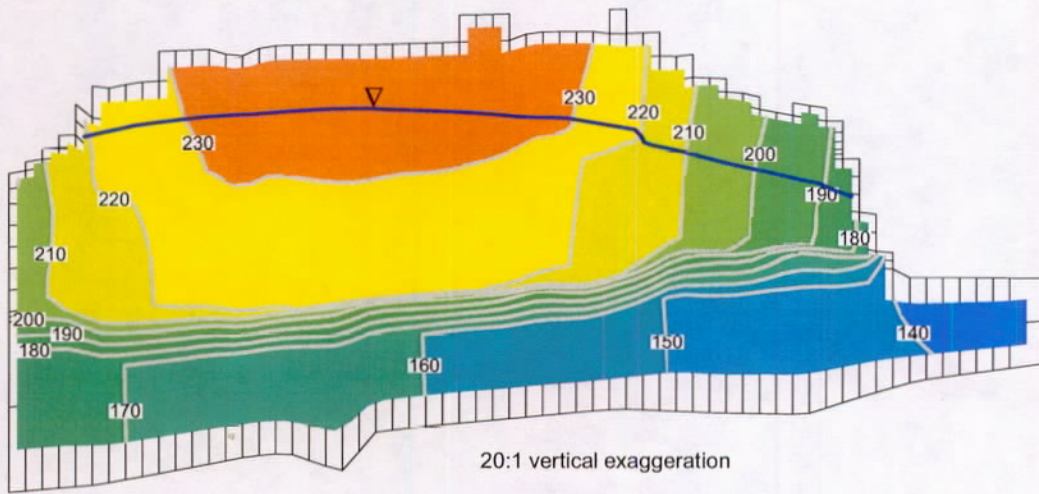


Figure 3-2. Simulated hydraulic head in GSA/PORFLOW model at cross-section through E Area (I=50).

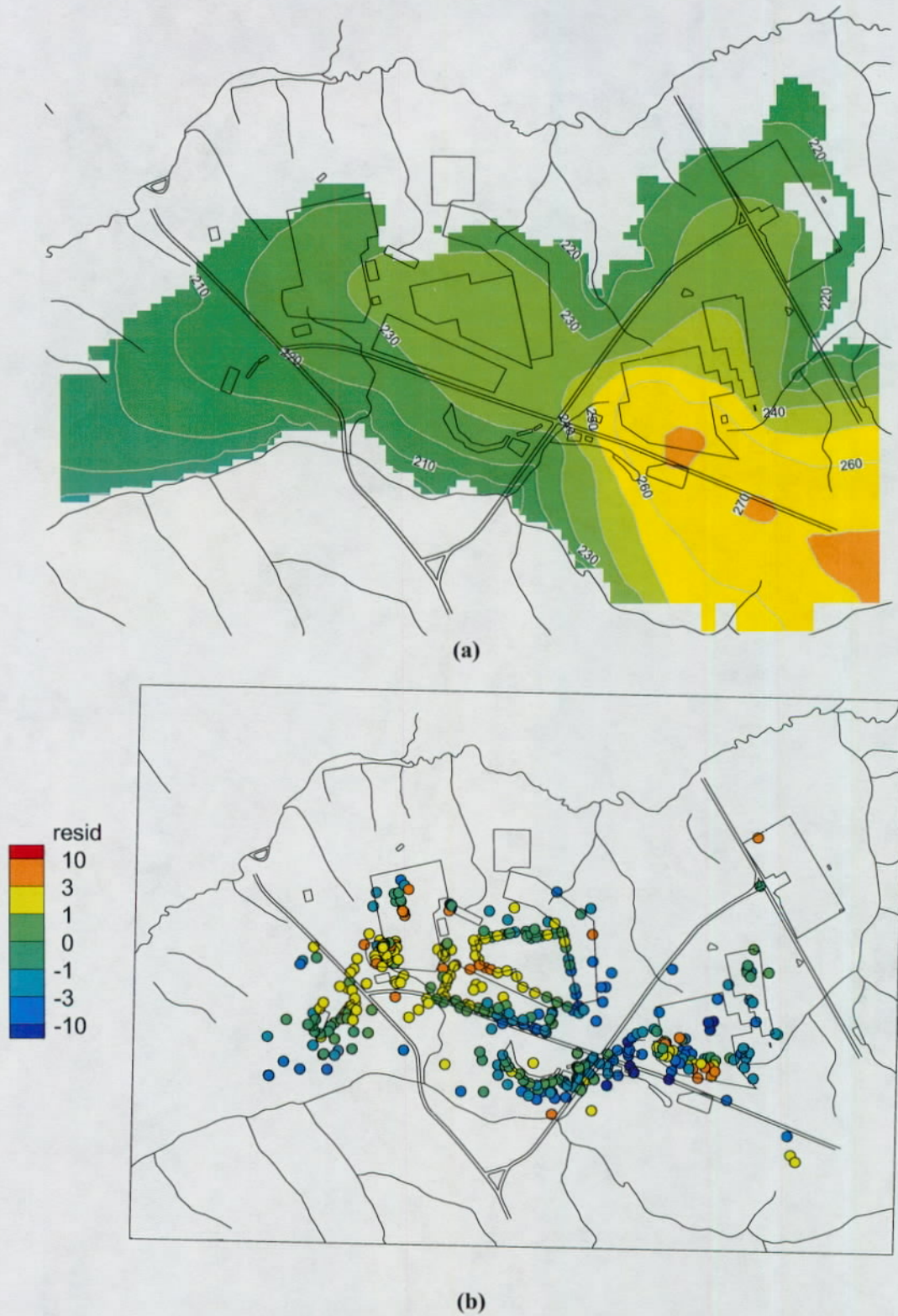


Figure 3-3. GSA/PORFLOW results for the UTR upper aquifer zone: (a) vertically-averaged head, and (b) residuals between computed and measured heads.

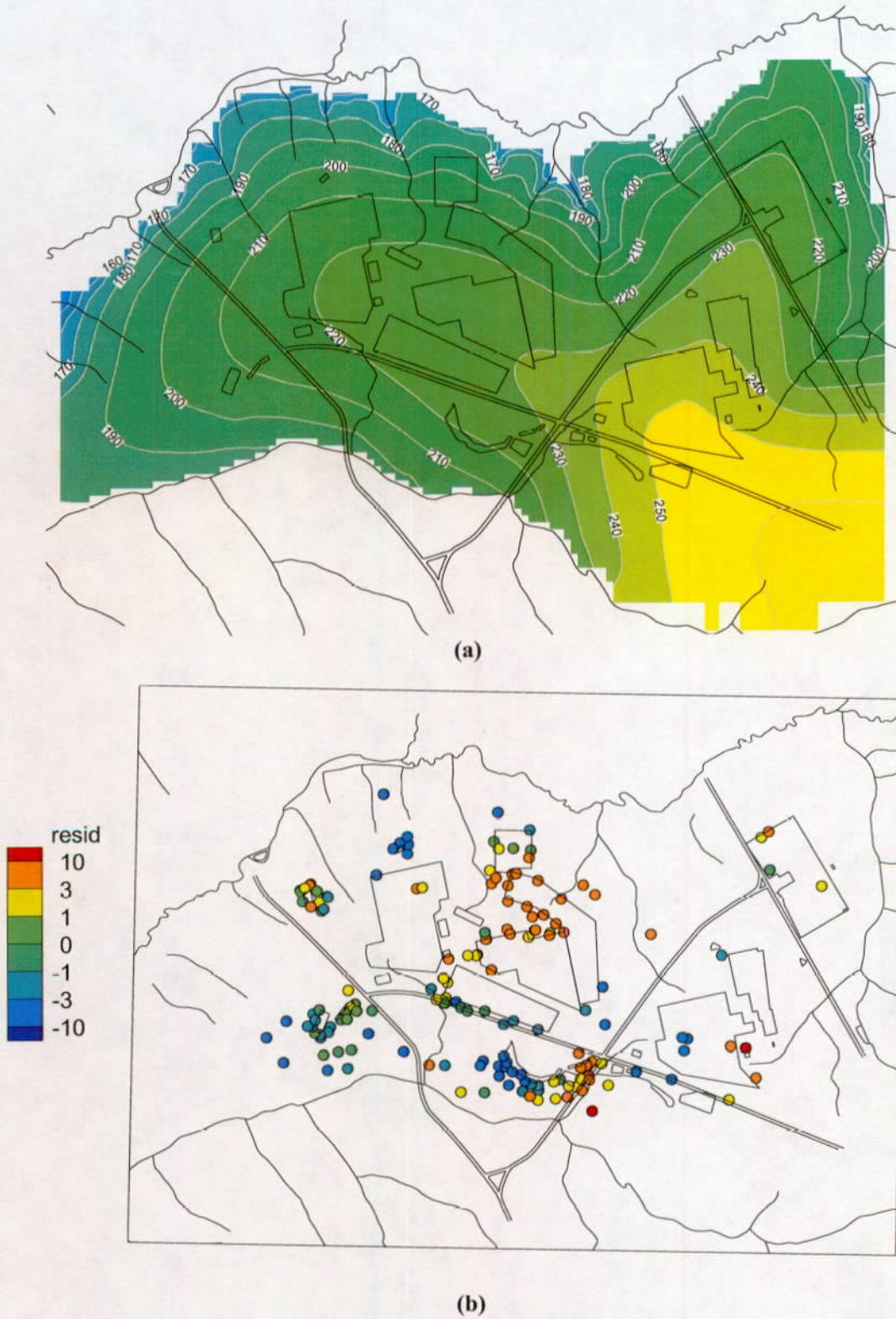
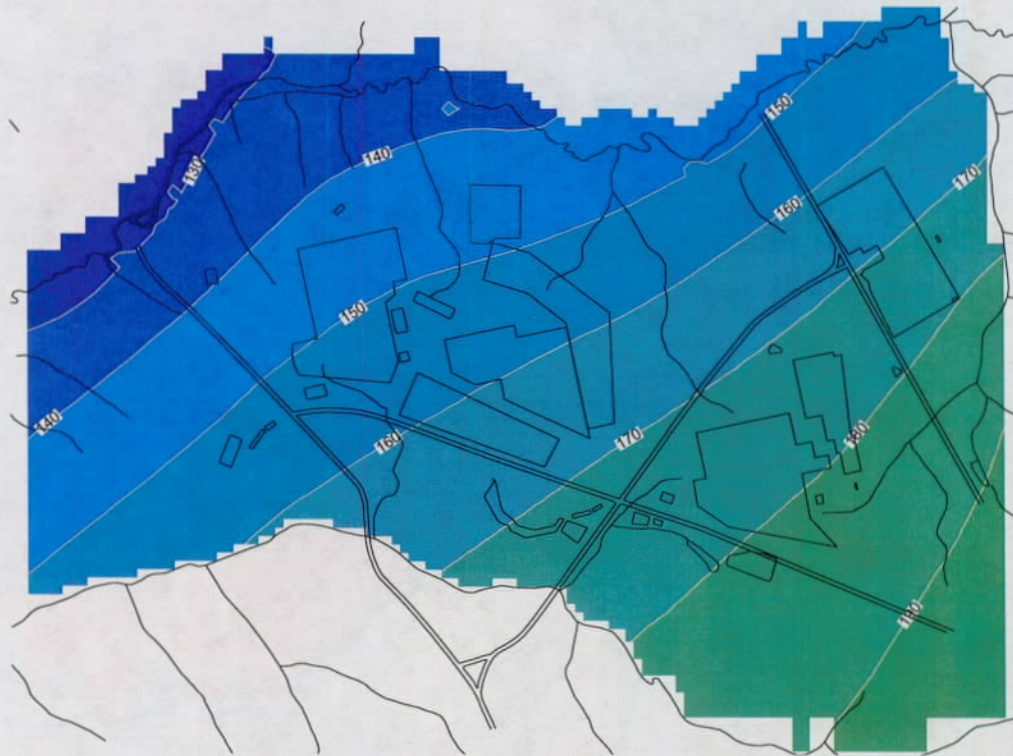
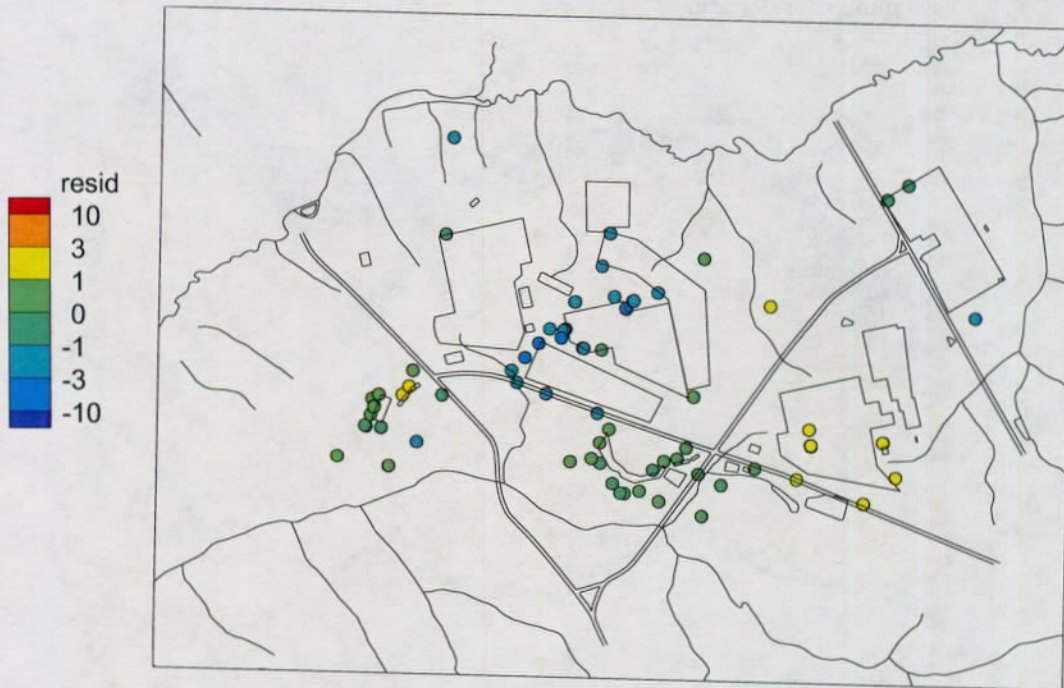


Figure 3-4. GSA/PORFLOW results for the UTR lower aquifer zone: (a) vertically-averaged head, and (b) residuals between computed and measured heads.



(a)



(b)

Figure 3-5. GSA/PORFLOW results for the Gordon aquifer unit: (a) vertically-averaged head, and (b) residuals between computed and measured heads.

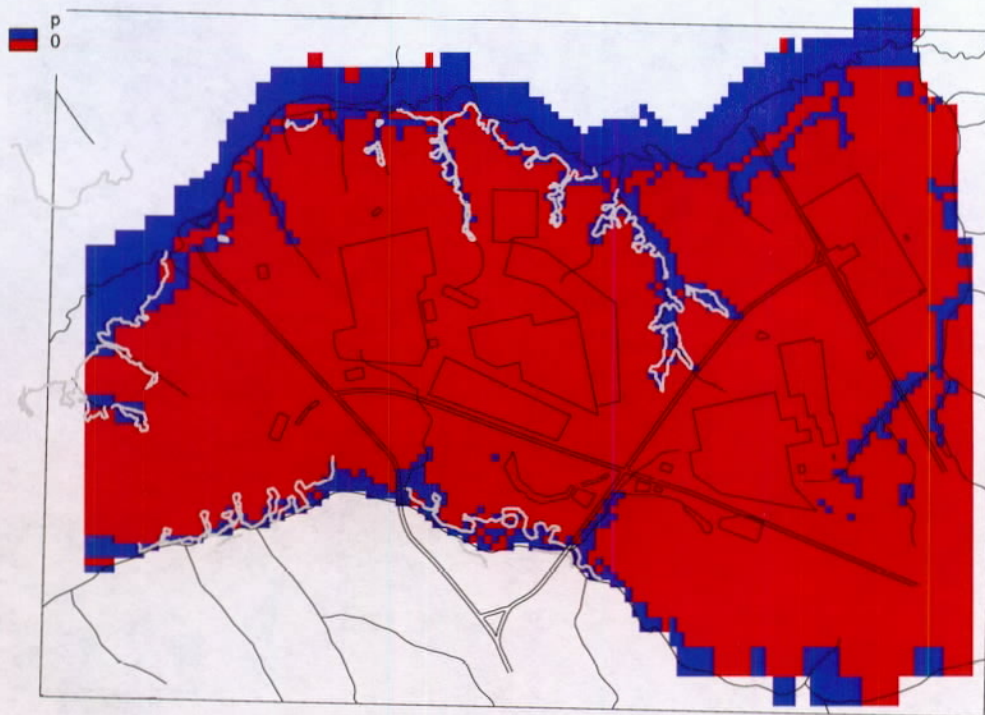


Figure 3-6. Simulated seepage areas in GSA/PORFLOW model compared to available seepage survey data.

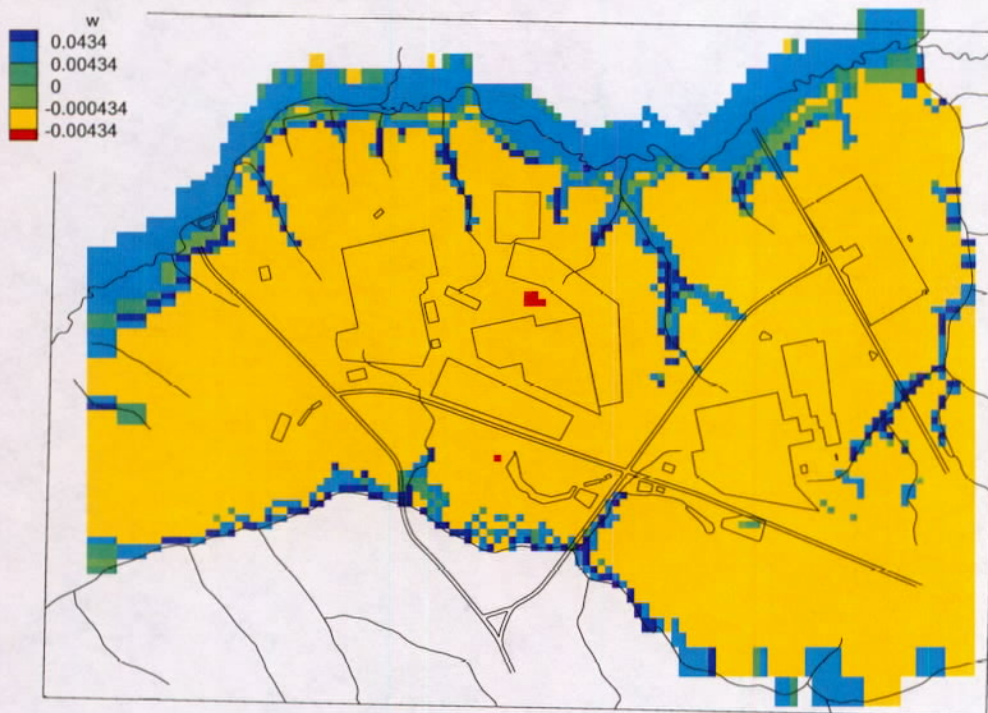


Figure 3-7. Simulated surface flux in GSA/PORFLOW model with positive values indicating groundwater discharge (ft³/d).

4.0 VERIFICATION AND VALIDATION

As used in this report, the term "verification" refers to confirmation that conceptual and/or mathematical models have been correctly implemented in software comprised of execution and input files. The GSA/PORFLOW model consists of a generic PORFLOW version 5.95.0 binary executable file and several ASCII input files to PORFLOW that define specific attributes of the GSA hydrologic system. "Validation" refers to confirmation that the software model is a valid representation of the physical system. Thus assuming a model has successfully undergone verification testing, validation emphasizes the broader question of whether the underlying conceptual and/or mathematical models adequately represent the actual hydrologic system. This section describes a sequence of V&V tests of the GSA/PORFLOW model. These include code-to-code comparisons between GSA/FACT and GSA/PORFLOW.

The PORFLOW Software Quality Assurance Plan is defined by Collard (2002). The document also contains acceptance testing results specific to PORFLOW version 4.00.7. The GSA/PORFLOW model results described in Section 3.0 were generated with PORFLOW version 5.95.0, thus acceptance testing for the newer PORFLOW code is required (Collard 2002, Sections 1.5.4 and 1.9.1 and p. 32). Under current plans, use of version 5.95.0 will be limited to generation of the steady-state GSA groundwater flow field described herein. Therefore, PORFLOW acceptance testing was limited to only those tests required to validate the steady-state flow field from the present application. Specifically, PORFLOW was tested to confirm that the code conserves mass and satisfies Darcy's Law, the governing equations embedded in PORFLOW. These two software V&V tests are described in the current report, a form of documentation permitted by the software QA plan (Collard 2002, p. 14). Additional V&V tests pertaining to the overall GSA/PORFLOW model follow.

4.1 Conservation of Mass

Under steady-state and constant fluid density conditions and no internal sources or sinks present, the net volumetric flow entering the model grid should be zero. A global mass balance is provided in Table 4-1. The discrepancy between incoming and outgoing flows (ft^3/d) is negligible at -0.04%. Under the same conditions, the net volumetric flow should also be effectively zero on a cell-by-cell basis. The results of mass balance computations for individual grid cells are summarized in Table 4-2. Discrepancies are few, small and presumably the result of incomplete model convergence.

Table 4-1. Global mass balance for GSA/PORFLOW model.

| BOUNDARY: | IN | OUT | NET FLOW | IN | OUT | NET FLUX |
|-----------|-----------|-----------|------------|-----------|-----------|------------|
| RECH01: | 1.220E+01 | 1.521E+01 | -3.006E+00 | 1.467E+01 | 1.828E+01 | -3.614E+00 |
| RECH02: | 1.125E-01 | 0.000E+00 | 1.125E-01 | 1.901E+01 | 0.000E+00 | 1.901E+01 |
| GENH01: | 5.940E-01 | 1.080E-03 | 5.929E-01 | 7.151E-01 | 1.300E-03 | 7.138E-01 |
| GENH02: | 4.619E-03 | 0.000E+00 | 4.619E-03 | 5.462E+00 | 0.000E+00 | 5.462E+00 |
| GENH05: | 1.030E-02 | 0.000E+00 | 1.030E-02 | 9.744E+01 | 0.000E+00 | 9.744E+01 |
| GENH10: | 1.590E-02 | 0.000E+00 | 1.590E-02 | 3.009E+01 | 0.000E+00 | 3.009E+01 |
| HEAD01: | 5.249E-02 | 4.039E-01 | -3.514E-01 | 5.710E+01 | 4.394E+02 | -3.823E+02 |
| HEAD02: | 3.819E+00 | 1.205E+00 | 2.613E+00 | 1.684E+02 | 5.314E+01 | 1.152E+02 |
| TOTALS: | 1.681E+01 | 1.682E+01 | -7.365E-03 | -0.04% | | |

Table 4-2. Summary of cell-by-cell mass balance for GSA/PORFLOW model.

| Description | Number | Percentage of total |
|---|--------|---------------------|
| Grid cells | 102295 | 100% |
| Cells with a flow imbalance exceeding 0.1% of largest magnitude flow among the 6 adjoining cell faces | 89 | 0.09% |
| Cells with a flow imbalance exceeding 0.1% of largest magnitude flow among all cell faces in the grid | 0 | 0% |

4.2 Darcy's Law

For a saturated porous medium and coordinate directions aligned with the principal axis of the conductivity tensor, Darcy's law for a particular coordinate axis can be expressed in terms of flowrate as

$$Q = qA = -KA \frac{dh}{dx} \quad (\text{Eq. 4-1})$$

where

Q = volumetric flow (L^3/T)

q = volumetric flux (L/T)

A = area normal to flow (L^2)

K = hydraulic conductivity (L/T)

h = hydraulic head (L)

x = distance in flow direction (L)

The precise numerical implementation of Eq. 4-1 is not defined in PORFLOW user documentation. Therefore, rigorous verification that Darcy's law as represented in PORFLOW is satisfied in GSA/PORFLOW is not readily attainable. Nevertheless, an independent calculation should be close to that embedded in PORFLOW and can serve as a validation test at a minimum.

Table 4-3 summarizes the results of such a calculation for cell faces in the saturated zone. The flowrate across each cell face was computed using a finite-difference version of Eq. 4-1 and geometric averaging to define conductivity at the face. This flowrate was compared to that reported by PORFLOW. The flowrates reported by PORFLOW and computed using Darcy's law are in general agreement. Discrepancies occur mostly at the Z- and Z+ faces of cells. At these locations the conductivity contrasts are often large (e.g. between aquifer and confining zones) and vertical mesh distortion creates ambiguities in the distance x . Thus the discrepancies are understandable. The comparison confirms that Darcy's law is satisfied.

Table 4-3. Summary of testing to confirm Darcy's law is satisfied at saturated internal cell faces.

| Description | Number | Percentage of total |
|---|---------|---------------------|
| Interior (non-boundary) cell faces in saturated zone | 239,562 | 100% |
| Faces with a flow imbalance exceeding 5% of largest magnitude flow among the 6 adjoining cell faces | 34,088 | 14% |
| Cells with a flow imbalance exceeding 1% of largest magnitude flow among all cell faces in the grid | 2382 | 1.0% |

4.3 Stratigraphy

Hydrostratigraphic surfaces, as represented in the GSA/PORFLOW model, are shown by flooded contours in Figures 4-1 through 4-5. The locations of individual picks used to create the surfaces are shown as scattered data, along with control data outside the model domain. The elevation of each pick is indicated by the color fill inside the outline of the symbol. Triangulation was used to interpolate the scattered picks onto layers of finite-element vertices (Flach 1999). Therefore, the interpolation is exact and color fill for the model surface and scattered data are observed to be identical. The GSA/PORFLOW stratigraphic surfaces are identical to those in the GSA/FACT model, which have previously been validated (Flach 1999, Figures 5.1.1 through 5.1.5 and Section 5.1). Figures 4-1 through 4-5 can also be validated through visual comparison to Figures 3 through 7 in Flach and Harris (1999), which are same surfaces developed in EarthVision using an alternative interpolation algorithm. The two sets of surfaces are observed to be similar.

4.4 Hydraulic Conductivity

The initial hydraulic conductivity field in the original GSA/FACT model was qualitatively validated against characterization data as described in Flach (1999, Section 5.5). The same comparison to field data is repeated in Appendix A for the calibrated GSA/PORFLOW model. The GSA/PORFLOW model conductivity field follows the trend indicated by slug and pump test data in 44% of the comparisons. That is, the model K field exhibits a higher (lower) than average value when the data exhibit a higher (lower) than average value. The model is counter to the data trend 17% of the time. Indeterminate or neutral comparisons comprise 39%. The former are cases in which the slug and pumping test data indicate opposing trends. Appendix A suggests that the calibrated GSA/PORFLOW conductivity field is valid in that it agrees or is neutral with respect to the data 83% of the time. These percentages are similar to those for the GSA/FACT model.

4.5 Hydraulic Head

Hydraulic head results from the GSA/PORFLOW model exhibit adequate agreement with well data considering uncertainties in the long-term average well water levels, limited characterization of field-scale conductivity, and the model resolution. Head residuals for GSA/PORFLOW are somewhat larger than those for GSA/FACT (Table 4-4) for various reasons. The artificial recharge zone in the GSA/FACT model was more effective in reducing head residuals near H Area, but is currently viewed as less realistic than the GSA/PORFLOW model. The coarser

vertical resolution of the GSA/PORFLOW mesh may also be a contributing factor. More extensive calibration efforts would likely improve the GSA/PORFLOW model.

Table 4-4. Summary statistics for hydraulic head residuals in GSA/FACT.

| Aquifer zone | Number | Median residual (ft) | Average residual (ft) | Root-mean-square residual (ft) | Minimum residual (ft) | Maximum residual (ft) |
|--------------|--------|-------------------------|--------------------------|-----------------------------------|--------------------------|--------------------------|
| Gordon | 79 | -1.2 | -1.8 | 2.5 | -6.2 | - |
| lower UTR | 172 | -0.4 | -0.1 | 4.8 | - | 16.0 |
| upper UTR | 407 | 0.0 | -0.3 | 2.6 | -9.8 | - |

4.6 Recharge and Stream Baseflows

The average recharge rate in the GSA/PORFLOW model, 14.7 in/yr, is about the same as the best-estimate based on field data, 15 in/yr. For comparison, the GSA/FACT model has an average rate of 14.5 in/yr. Stream baseflows are similar for the two models, with the largest differences occurring for Upper Three Runs and McQueen Branch (Table 4-5). The GSA/PORFLOW model prediction for McQueen Branch (2.4 ft³/s) is significantly closer to the prior estimate (1.5 ft³/s) than the GSA/FACT model (3.6 ft³/s). Conversely, the GSA/PORFLOW model prediction for Upper Three Runs (11.4 ft³/s) is deviates further from the prior estimate (18.2 ft³/s) than the GSA/FACT model (14.5 ft³/s).

The GSA/PORFLOW model prediction of seepage faces is approximately the same as past survey data (Figure 3-6). The resolution of seepage faces and seeplines is poorer for GSA/PORFLOW compared to the GSA/FACT model. The top surface of the latter conforms to the actual ground surface more accurately.

Table 4-5. Comparison of measured and simulated stream baseflow in GSA/FACT.

| Stream | Estimated baseflow contribution from GSA (ft ³ /s) | Simulated baseflow contribution from GSA (ft ³ /s) |
|---|--|--|
| Upper Three Runs and tributaries excluding McQueen Branch | 18.2 | 14.5 |
| Fourmile Branch and tributaries | 2.6 | 3.6 |
| McQueen Branch | 1.5 | 4.7 |
| Crouch Branch | 1.8 | 1.6 |

4.7 Particle Tracking and Solute Transport

Figure 4-6 compares particle tracking simulations based on the velocity fields from GSA/FACT and GSA/PORFLOW, as a V&V test of GSA/PORFLOW through code-to-code comparison. Overall, particle trajectories and timing are close between the two models. Locally, differences can be more significant.

Flach and Millings (2003) recently performed tritium transport simulations for several pairs of LAW vault footprints in E Area using the GSA/FACT flow field. Table 4-6 summarizes the peak groundwater concentration results from those computer runs, and analogous simulations performed using the GSA/PORFLOW flow field. The transport simulations for both flow fields were performed with PORFLOW using the identical contaminant source and transport parameters. On average the peak concentration results are about the same. However, individual runs tend to vary on the order of $\pm 25\%$.

The particle tracking and solute transport comparison indicates the velocity field is similar between the two models.

Table 4-6. Tritium transport simulations for various LAW vault footprints following Flach and Millings (2003).

H-3

| Peak conc. at 100 meter well (any location) | | | | GSA/FACT | | Tecplot Tecplot Tecplot -PORFLOW | | | | | GSA/PORFLOW | | |
|---|-----------------|----|----|-----------|-----------|----------------------------------|----|----|----|------|-------------|-----------|----------|
| Case | Peak conc. node | | | Peak time | Peak conc | Peak conc. node | | | | | Peak time | Peak conc | Conc. |
| | I | J | K | (yrs) | (pCi/L) | N | i | j | k | Keqv | (yrs) | (pCi/L) | vs. FACT |
| PA | 36 | 24 | 9 | 9 | 1.59E+03 | | | | | | | | |
| Case01 | 36 | 24 | 11 | 9 | 2785 | 65772 | 55 | 51 | 11 | 12 | 9 | 3153 | 1.13 |
| Case02 | 37 | 23 | 12 | 10 | 3145 | 71174 | 56 | 50 | 12 | 13 | 9 | 3027 | 0.96 |
| Case03 | 41 | 21 | 11 | 10 | 2411 | 59907 | 60 | 48 | 10 | 11 | 10 | 1816 | 0.75 |
| Case04 | 43 | 19 | 12 | 10 | 2369 | 59717 | 62 | 46 | 10 | 11 | 11 | 1574 | 0.66 |
| Case05 | 43 | 15 | 13 | 12 | 2195 | 75584 | 63 | 40 | 13 | 14 | 11 | 1946 | 0.89 |
| Case06 | 44 | 12 | 14 | 12 | 1788 | 80508 | 64 | 37 | 14 | 15 | 11 | 1891 | 1.06 |
| Case07 | 44 | 10 | 14 | 12 | 2183 | 80408 | 64 | 36 | 14 | 15 | 12 | 1915 | 0.88 |
| Case08 | 42 | 17 | 13 | 11 | 2848 | 70603 | 61 | 44 | 12 | 13 | 11 | 2454 | 0.86 |
| Case09 | 42 | 16 | 13 | 11 | 2923 | 70502 | 61 | 43 | 12 | 13 | 11 | 2206 | 0.75 |
| Case10 | 44 | 13 | 14 | 11 | 5812 | 75584 | 63 | 40 | 13 | 14 | 12 | 5330 | 0.92 |

0.88 avg

| Peak conc. within aquifer zone only | | | | GSA/FACT | | Tecplot Tecplot Tecplot -PORFLOW | | | | | GSA/PORFLOW | | |
|-------------------------------------|-----------------|----|----|-----------|-----------|----------------------------------|----|----|----|------|-------------|-----------|----------|
| Case | Peak conc. node | | | Peak time | Peak conc | Peak conc. node | | | | | Peak time | Peak conc | Conc. |
| | I | J | K | (yrs) | (pCi/L) | N | i | j | k | Keqv | (yrs) | (pCi/L) | vs. FACT |
| PA | 36 | 24 | 9 | 9 | 1.59E+03 | | | | | | | | |
| Case01 | 36 | 24 | 10 | 10 | 2248 | 54516 | 55 | 51 | 9 | 10 | 10 | 2095 | 0.93 |
| Case02 | 37 | 23 | 10 | 12 | 1595 | 71174 | 56 | 50 | 12 | 13 | 9 | 3027 | 1.90 |
| Case03 | 41 | 21 | 10 | 12 | 1783 | 54227 | 60 | 48 | 9 | 10 | 11 | 1522 | 0.85 |
| Case04 | 43 | 19 | 10 | 12 | 1171 | 54031 | 62 | 46 | 9 | 10 | 12 | 1177 | 1.01 |
| Case05 | 43 | 15 | 13 | 12 | 2195 | 75584 | 63 | 40 | 13 | 14 | 11 | 1946 | 0.89 |
| Case06 | 44 | 12 | 14 | 12 | 1788 | 80508 | 64 | 37 | 14 | 15 | 11 | 1891 | 1.06 |
| Case07 | 44 | 10 | 14 | 12 | 2183 | 80408 | 64 | 36 | 14 | 15 | 12 | 1915 | 0.88 |
| Case08 | 42 | 17 | 13 | 11 | 2848 | 70603 | 61 | 44 | 12 | 13 | 11 | 2454 | 0.86 |
| Case09 | 42 | 16 | 13 | 11 | 2923 | 70502 | 61 | 43 | 12 | 13 | 11 | 2206 | 0.75 |
| Case10 | 44 | 13 | 14 | 11 | 5812 | 75584 | 63 | 40 | 13 | 14 | 12 | 5330 | 0.92 |

1.01 avg

4.8 Summary Assessment

The GSA/PORFLOW model conserves mass, satisfies Darcy's law, and produces simulated hydraulic heads and groundwater flows that substantially agree with extensive field data. GSA/PORFLOW particle tracking and solute transport results are similar to those produced by GSA/FACT. Thus the new PORFLOW model appears to produce valid simulations of groundwater flow in the GSA.



Figure 4-1. GSA/PORFLOW representation of the top of the Meyers Branch confining system (Crouch Branch confining unit).

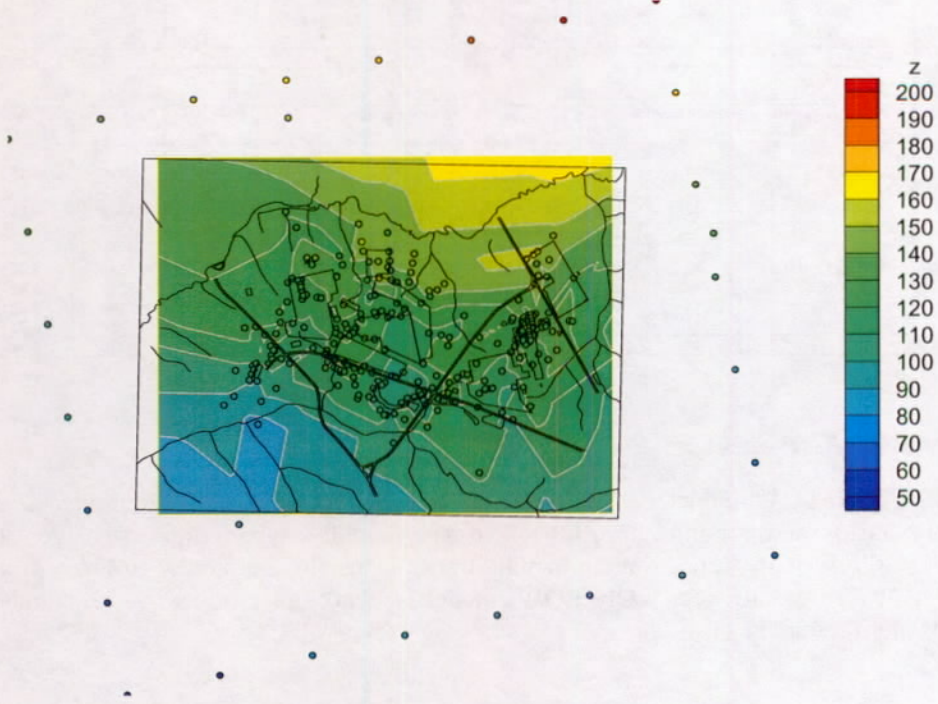


Figure 4-2. GSA/PORFLOW representation of the top of the Gordon aquifer unit.

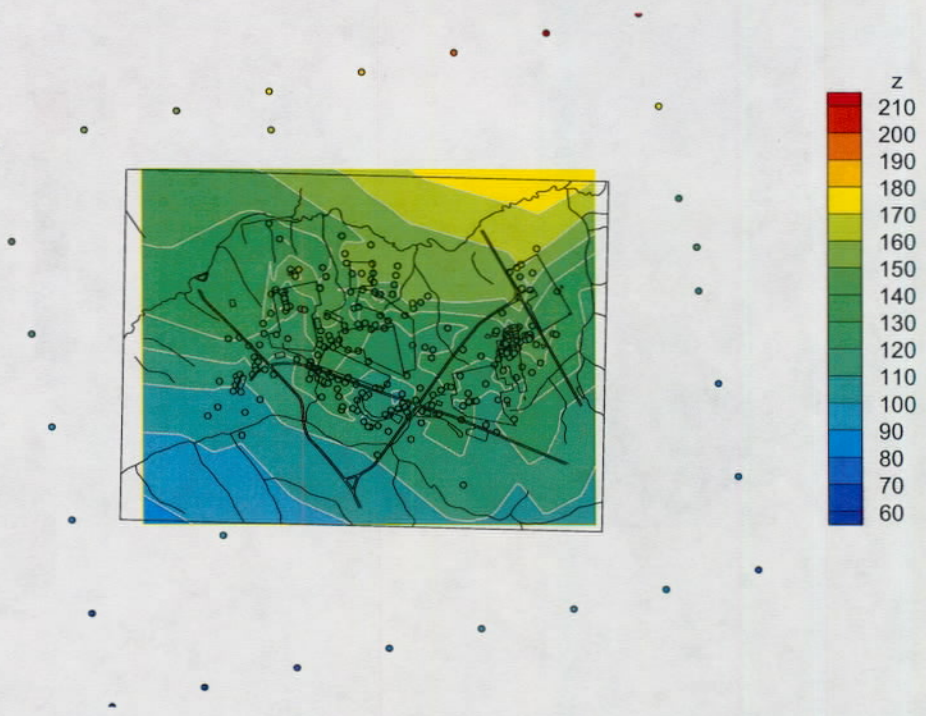


Figure 4-3. GSA/PORFLOW representation of the top of the Gordon confining unit.

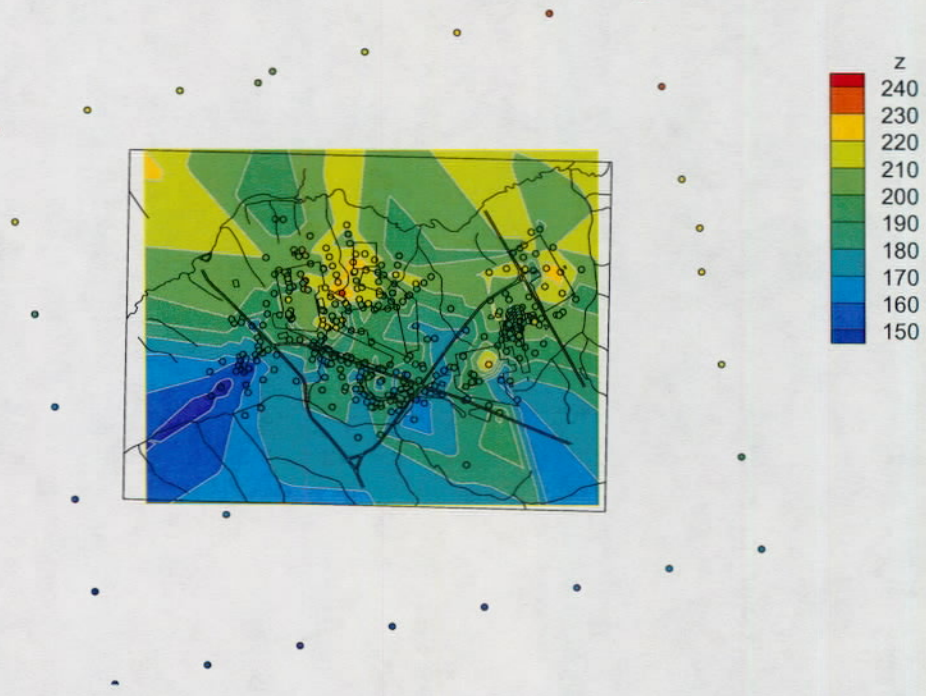


Figure 4-4. GSA/PORFLOW representation of the top of the UTR lower aquifer zone.

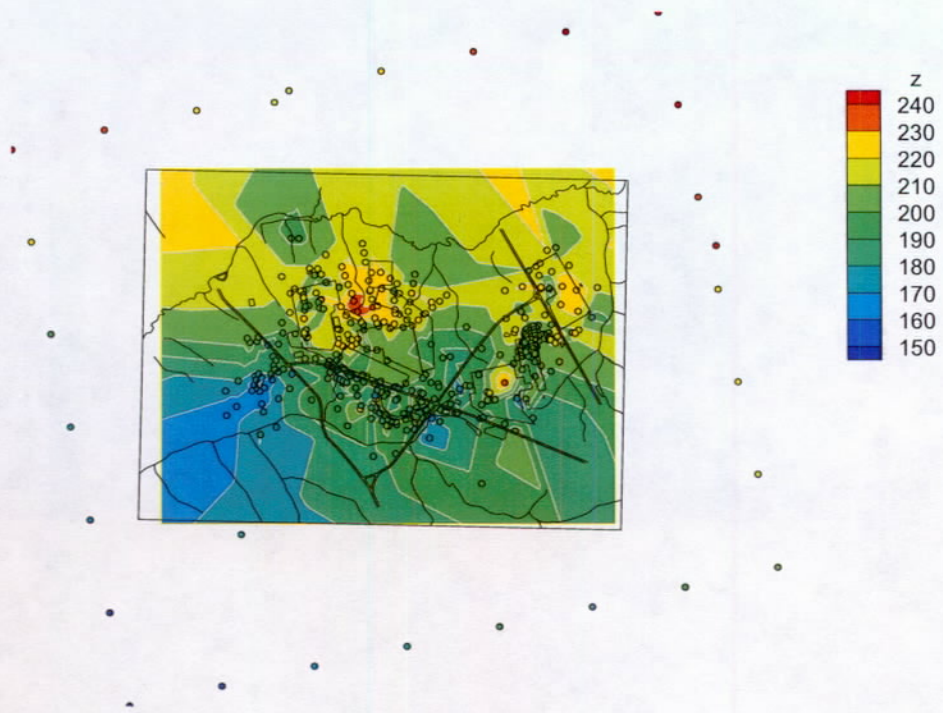
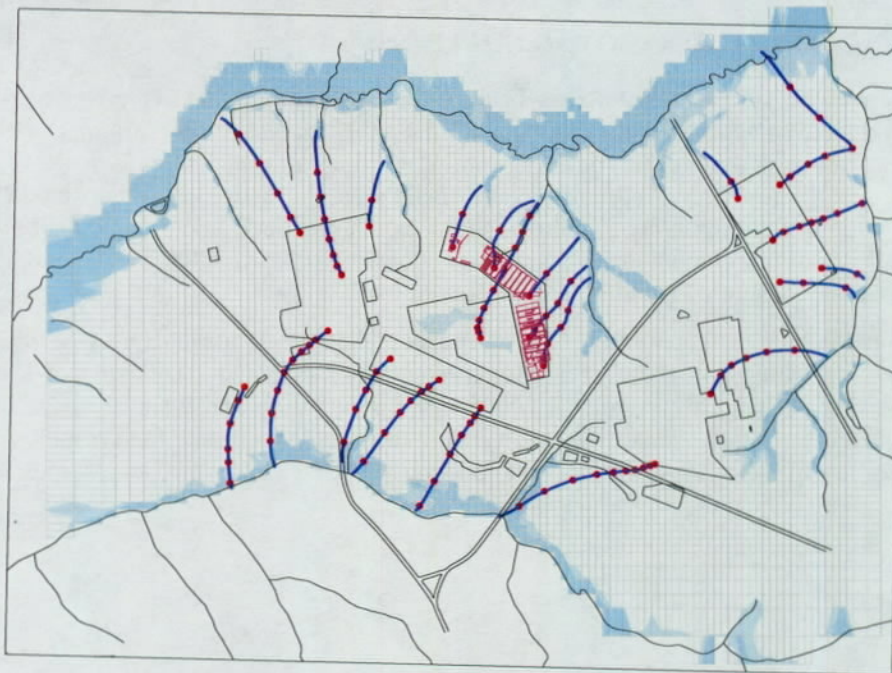
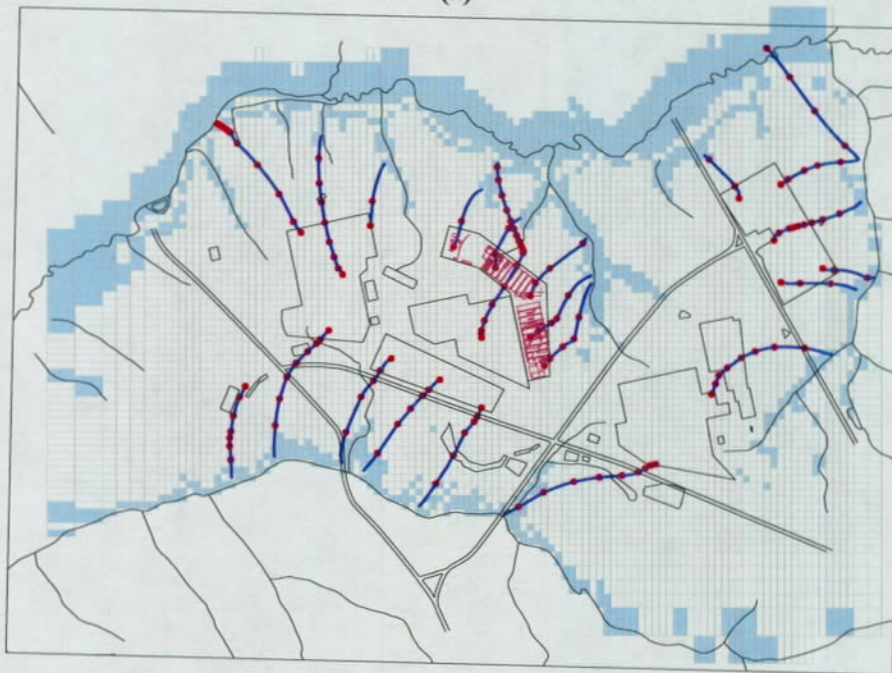


Figure 4-5. GSA/PORFLOW representation of the top of the UTR tan clay confining zone.



(a)



(b)

Figure 4-6. Particle tracking simulation with 5 year markers for (a) GSA/FACT and (b) GSA/PORFLOW.

5.0 CONCLUSIONS AND RECOMMENDATIONS

A numerical model of groundwater flow beneath the GSA using PORFLOW version 5.95.0 has been developed based on the former GSA/FACT model. The original GSA/FACT characterization and monitoring datasets, pre-processing algorithms, and model calibration strategies were largely preserved. Differences in flow results between the two models, due to mesh and code differences, were minimized to the extent practical. The GSA/PORFLOW model is an equally valid representation of groundwater flow compared to GSA/FACT, and suitable as the new baseline for future Performance Assessment work.

Software acceptance testing of PORFLOW version 5.95.0 used to generate GSA/PORFLOW results was very limited in scope: Tests for mass conservation and satisfaction of Darcy's law were performed. These tests, combined with visual confirmation that boundary conditions have been adequately specified, are sufficient to validate the steady-state flow field results. Additional software testing would be required for other applications of PORFLOW version 5.95.0.

THIS PAGE INTENTIONALLY LEFT BLANK

6.0 REFERENCES

- Analytic & Computational Research, Inc. 1994. *Validation; Version 2.50*, Bel Air, California.
- Analytic & Computational Research, Inc. 2000. *PORFLOW User's Manual; Version 4.00 Rev: 4*, Bel Air, California.
- Collard, L. 2002. *Software Quality Assurance Plan for the PORFLOW Code*, WSRC-SQP-A-00028, Westinghouse Savannah River Company, Aiken, South Carolina.
- Flach, G.P. 1999. *Pre- and Post-Processing Software Associated with the GSA/FACT Groundwater Flow Model (U)*, WSRC-TR-99-00106 Rev. 0, Westinghouse Savannah River Company, Aiken, South Carolina.
- Flach, G.P., and Harris, M.K. 1997. *Integrated Hydrogeological Model of the General Separations Area (U); Volume 2: Groundwater Flow Model (U)*, WSRC-TR-96-0399 Rev. 0, Westinghouse Savannah River Company, Aiken, South Carolina.
- Flach, G.P., and Harris, M.K. 1999. *Integrated Hydrogeological Model of the General Separations Area (U); Volume 2: Groundwater Flow Model (U)*, WSRC-TR-96-0399 Rev. 1, Westinghouse Savannah River Company, Aiken, South Carolina.
- Flach, G. P., and Millings, M. R. 2003. *Unreviewed Disposal Question; Evaluation of Unanalyzed Slit and Engineered Trench Locations*, WSRC-TR-2003-00432, Rev. 0, Westinghouse Savannah River Company, Aiken, South Carolina.
- Hamm, L.L., and Aleman, S.E. 2000. *FACT (Version 2.0); Subsurface Flow and Contaminant Transport Documentation and User's Guide (U)*, WSRC-TR-99-00282, Westinghouse Savannah River Company, Aiken, South Carolina.
- McDowell-Boyer, L., Yu, A.D., Cook, J.R., Kocher, D.C., Wilhite, E.L., Holmes-Burns, H., and Young, K.E. 2000. *Radiological Performance Assessment for the E-Area Low-Level Waste Facility*, WSRC-RP-94-218, Revision 1, Westinghouse Savannah River Company, Aiken, South Carolina.

THIS PAGE INTENTIONALLY LEFT BLANK

**APPENDIX A - QUALITATIVE COMPARISON OF GSA/PORFLOW HORIZONTAL
CONDUCTIVITY FIELD TO CHARACTERIZATION DATA.**

**Table A-1. Comparison of characterization data trends for horizontal conductivity
to GSA/PORFLOW variations from average.**

| (1) Well ID | (2) z bot (ft) | (3) z top (ft) | (4) %sand | (5) slug Kh (ft/d) | (6) pump Kh (ft/d) | (7) modl Kh (ft/d) | (8) sand trend | (9) slug trend | (10) pump trend | (11) model trend | (12) Agree/ Dis- agree |
|----------------|----------------------|----------------------|--------------|-----------------------------|-----------------------------|-----------------------------|----------------------|----------------------|-----------------------|------------------------|---------------------------------|
| BGC001A | 108 | 112 | -1 | 0.46 | -1 | 0.32 | - | L | - | L | A |
| BGC002A | 117.6 | 121.6 | -1 | 0.02 | -1 | 3.37 | - | L | - | L | A |
| BGC003A | 131.6 | 135.6 | -1 | 15.9 | -1 | 11.39 | - | H | - | H | A |
| BGO001D | 225 | 245 | 0.83 | 0.31 | -1 | 10.56 | H | L | - | H | - |
| BGO002D | 218.9 | 238.9 | -1 | 0.62 | -1 | 6.46 | - | L | - | L | A |
| BGO003A | 103.7 | 113.7 | 0.82 | 4.22 | -1 | 16.58 | H | H | - | H | A |
| BGO003C | 178.7 | 188.7 | 0.83 | 0.01 | -1 | 1.44 | H | L | - | L | - |
| BGO003D | 227.6 | 247.6 | 0.71 | 0.14 | -1 | 6.21 | L | L | - | L | A |
| BGO004D | 220.6 | 240.6 | -1 | 0.69 | -1 | 9.65 | - | L | - | L | A |
| BGO005C | 183.2 | 193.2 | 0.79 | 0.13 | -1 | 7.66 | H | L | - | L | - |
| BGO005D | 219.3 | 239.3 | 0.84 | 0.73 | -1 | 8.41 | H | L | - | L | - |
| BGO006A | 107.5 | 117.5 | 0.9 | 0.77 | -1 | 4.37 | H | L | - | L | - |
| BGO006C | 158 | 168 | 0.71 | 1.51 | -1 | 10.71 | L | L | - | H | D |
| BGO006D | 217.2 | 237.2 | 0.89 | 0.38 | -1 | 10.99 | H | L | - | H | - |
| BGO007D | 220.2 | 240.2 | -1 | 15.1 | -1 | 12.97 | - | H | - | H | A |
| BGO008A | 105.3 | 115.3 | 0.76 | 0.21 | -1 | 9.72 | L | L | - | L | A |
| BGO008AR | 94.6 | 104.6 | 0.91 | 0.9 | -1 | 9.72 | H | L | - | L | - |
| BGO008C | 174.3 | 184.3 | 0.9 | 1.39 | 0.41 | 8.53 | H | L | L | L | A |
| BGO008D | 220.6 | 240.6 | 0.89 | 1.87 | 1.25 | 13.31 | H | L | L | H | D |
| BGO009D | 209.2 | 229.2 | 0.7 | 0.1 | -1 | 7.02 | L | L | - | L | A |
| BGO010A | 111.1 | 121.1 | 0.88 | 0.16 | -1 | 8.38 | H | L | - | L | - |
| BGO010AA | 80.8 | 90.8 | 0.63 | 0.43 | -1 | 7.92 | L | L | - | L | A |
| BGO010AR | 96.5 | 106.5 | 0.9 | 0.85 | -1 | 8.38 | H | L | - | L | - |
| BGO010B | 139 | 149 | 0.61 | 0.31 | -1 | 1.85 | L | L | - | L | A |
| BGO010C | 157.3 | 167.3 | 0.69 | 0.07 | -1 | 5.51 | L | L | - | L | A |
| BGO010D | 230.5 | 250.5 | 0.83 | 0.33 | -1 | 9.03 | H | L | - | L | - |
| BGO010DR | 218.3 | 238.3 | 0.8 | 1.16 | -1 | 10.01 | H | L | - | L | - |
| BGO011D | 216.3 | 236.3 | -1 | 2.54 | 1.89 | 8.84 | - | L | L | L | A |
| BGO012A | 106.4 | 116.4 | 0.89 | 0 | -1 | 4.99 | H | L | - | L | - |
| BGO012AR | 99.3 | 109.3 | 0.89 | 0.98 | -1 | 4.99 | H | L | - | L | - |

| (1) Well ID | (2) z bot (ft) | (3) z top (ft) | (4) %sand | (5) slug Kh (ft/d) | (6) pump Kh (ft/d) | (7) modl Kh (ft/d) | (8) sand trend | (9) slug trend | (10) pump trend | (11) model trend | (12) Agree/ Dis- agree |
|----------------|----------------------|----------------------|--------------|-----------------------------|-----------------------------|-----------------------------|----------------------|----------------------|-----------------------|------------------------|---------------------------------|
| BGO012C | 153.6 | 163.6 | 0.93 | 0.57 | -1 | 7.77 | H | L | - | L | - |
| BGO012CR | 144 | 154 | 0.92 | 0.16 | -1 | 7.33 | H | L | - | L | - |
| BGO012D | 217.8 | 237.8 | 0.87 | 0.12 | -1 | 9.22 | H | L | - | L | - |
| BGO013D | 228.5 | 248.5 | -1 | 0.14 | -1 | 6.91 | - | L | - | L | A |
| BGO013DR | 210.3 | 220.3 | -1 | 0.28 | -1 | 9.95 | - | L | - | L | A |
| BGO014A | 109.6 | 119.6 | 0.87 | 0.04 | -1 | 5.65 | H | L | - | L | - |
| BGO014AR | 96.8 | 106.8 | 0.88 | 1.65 | -1 | 6.58 | H | L | - | L | - |
| BGO014C | 192.1 | 202.1 | 0.84 | 0.98 | 0.89 | 7.76 | H | L | L | L | A |
| BGO014CR | 190.1 | 200.1 | 0.82 | 0.4 | -1 | 7.86 | H | L | - | L | - |
| BGO014D | 229.6 | 249.6 | 0.77 | 0.56 | -1 | 6.12 | L | L | - | L | A |
| BGO014DR | 218.1 | 238.1 | 0.74 | 2.15 | -1 | 11.05 | L | L | - | H | D |
| BGO015D | 218.7 | 238.7 | -1 | 1.11 | -1 | 6.12 | - | L | - | L | A |
| BGO016A | 102.5 | 112.5 | 0.94 | 0.15 | -1 | 8.25 | H | L | - | L | - |
| BGO016D | 217.3 | 237.3 | 0.67 | 0.07 | -1 | 4.99 | L | L | - | L | A |
| BGO017D | 204 | 224 | -1 | 1.28 | -1 | 9.75 | - | L | - | L | A |
| BGO018A | 99.5 | 109.5 | 0.91 | 12 | -1 | 16.69 | H | H | - | H | A |
| BGO018D | 219.6 | 239.6 | 0.78 | 12.6 | -1 | 14.24 | L | H | - | H | - |
| BGO019D | 196.8 | 216.8 | -1 | 0.45 | -1 | 7.68 | - | L | - | L | A |
| BGO020B | 131 | 141 | 0.83 | 0.38 | -1 | 8.09 | H | L | - | L | - |
| BGO020C | 174 | 184 | 0.83 | 0.94 | -1 | 10.23 | H | L | - | H | - |
| BGO021D | 217.7 | 237.7 | 0.73 | 0.79 | -1 | 5.49 | L | L | - | L | A |
| BGO023D | 222 | 242 | 0.79 | 1.11 | -1 | 8.03 | H | L | - | L | - |
| BGO024D | 221 | 241 | -1 | 0.36 | -1 | 7.83 | - | L | - | L | A |
| BGO025A | 104.1 | 114.1 | 0.89 | 0.5 | -1 | 7.22 | H | L | - | L | - |
| BGO029C | 176.8 | 186.8 | 0.69 | 0.29 | -1 | 8.34 | L | L | - | L | A |
| BGO029D | 208.5 | 228.5 | 0.89 | 1.58 | -1 | 11.06 | H | L | - | H | - |
| BGO041A | 103.3 | 113.3 | 0.9 | 0.13 | -1 | 9.09 | H | L | - | L | - |
| BGO042C | 185.9 | 195.9 | 0.91 | 0.45 | -1 | 10.3 | H | L | - | H | - |
| BGO043AA | 62.2 | 72.2 | 0.86 | 0.86 | -1 | 10.31 | H | L | - | H | - |
| BGO044A | 98 | 108 | 0.93 | 4.03 | -1 | 10.06 | H | L | - | H | - |
| BGO044AA | 61.2 | 71.3 | 0.86 | 4.37 | -1 | 13.07 | H | H | - | H | A |
| BGO044B | 148.1 | 158.1 | 0.73 | 0.06 | -1 | 4.43 | L | L | - | L | A |
| BGO044C | 190.6 | 200.6 | 0.82 | 0.08 | -1 | 7.39 | H | L | - | L | - |
| BGO044D | 223.4 | 233.4 | 0.83 | 13 | -1 | 11.32 | H | H | - | H | A |
| BGO045A | 116.9 | 126.9 | 0.91 | 2.45 | -1 | 4.48 | H | L | - | L | - |

| (1) Well ID | (2) z bot (ft) | (3) z top (ft) | (4) %sand | (5) slug Kh (ft/d) | (6) pump Kh (ft/d) | (7) modl Kh (ft/d) | (8) sand trend | (9) slug trend | (10) pump trend | (11) model trend | (12) Agree/ Dis- agree |
|----------------|----------------------|----------------------|--------------|-----------------------------|-----------------------------|-----------------------------|----------------------|----------------------|-----------------------|------------------------|---------------------------------|
| BGO045B | 137 | 147 | 0.9 | 0.12 | -1 | 7.94 | H | L | - | L | - |
| BGO045C | 190.5 | 200.5 | 0.7 | 1.22 | -1 | 0.01 | L | L | - | L | A |
| BGO045D | 209.6 | 229.6 | 0.9 | 6.07 | -1 | 14.56 | H | H | - | H | A |
| BGO046B | 140.4 | 150.4 | 0.88 | 2.33 | -1 | 12.6 | H | L | - | H | - |
| BGO046C | 178 | 188 | 0.86 | 0.14 | -1 | 8.22 | H | L | - | L | - |
| BGO046D | 202.1 | 212.1 | 0.88 | 11.5 | -1 | 14.98 | H | H | - | H | A |
| BGO047A | 86.8 | 96.8 | 0.95 | 3.06 | -1 | 13.87 | H | L | - | H | - |
| BGO047C | 178.6 | 188.6 | 0.86 | 0.46 | -1 | 9.64 | H | L | - | L | - |
| BGO047D | 203.4 | 213.4 | 0.91 | 15.9 | -1 | 15.32 | H | H | - | H | A |
| BGO048C | 176.7 | 186.7 | 0.92 | 2.15 | -1 | 10.39 | H | L | - | H | - |
| BGO048D | 202 | 212 | 0.75 | 11 | -1 | 13.88 | L | H | - | H | - |
| BGO049A | 75.1 | 85.1 | 0.93 | 0.48 | -1 | 10.83 | H | L | - | H | - |
| BGO049C | 166 | 176 | 0.91 | 0.88 | -1 | 11.19 | H | L | - | H | - |
| BGO049D | 218.5 | 238.5 | 0.87 | 0.73 | -1 | 9 | H | L | - | L | - |
| BGO050A | 90.5 | 100.5 | 0.89 | 0.4 | -1 | 10.84 | H | L | - | H | - |
| BGO050C | 162.5 | 172.5 | 0.77 | 0.33 | -1 | 9.08 | L | L | - | L | A |
| BGO050D | 208 | 228 | 0.83 | 1.61 | -1 | 11.42 | H | L | - | H | - |
| BGO051A | 75.1 | 85.1 | 0.91 | 10.5 | -1 | 18.21 | H | H | - | H | A |
| BGO051AA | 29.2 | 39.2 | 0.67 | 0.99 | -1 | 8.17 | L | L | - | L | A |
| BGO051B | 117.1 | 127.1 | 0.82 | 5.39 | -1 | 2.9 | H | H | - | L | D |
| BGO051C | 175.1 | 185.1 | 0.87 | 1.51 | -1 | 12.6 | H | L | - | H | - |
| BGO051D | 220 | 240.1 | 0.82 | 0.24 | -1 | 6.81 | H | L | - | L | - |
| BGO052A | 81.7 | 91.7 | 0.89 | 4.15 | -1 | 17.23 | H | H | - | H | A |
| BGO052AA | 36.6 | 46.6 | 0.9 | 4.52 | -1 | 12.24 | H | H | - | H | A |
| BGO052B | 126.7 | 136.7 | 0.82 | 0.53 | -1 | 7.08 | H | L | - | L | - |
| BGO052C | 178.7 | 188.7 | 0.79 | 2.69 | -1 | 12.46 | H | L | - | H | - |
| BGO052D | 219.4 | 239.4 | 0.76 | 0.11 | -1 | 5.14 | L | L | - | L | A |
| BGO053A | 78.6 | 88.6 | 0.95 | 0.36 | -1 | 9.13 | H | L | - | L | - |
| BGO053AA | 38.8 | 48.8 | 0.96 | 1.12 | -1 | 12.15 | H | L | - | H | - |
| BGO053B | 143.4 | 153.4 | 0.88 | 0.11 | -1 | 6.21 | H | L | - | L | - |
| BGO053C | 183.1 | 193.1 | 0.93 | 2.3 | -1 | 9.76 | H | L | - | L | - |
| BGO053D | 225.2 | 245.2 | 0.87 | 1.94 | -1 | 12.18 | H | L | - | H | - |
| BGX001A | 114.1 | 124.1 | 0.93 | 0.01 | -1 | 6.23 | H | L | - | L | - |
| BGX001C | 176 | 186 | 0.85 | 0.36 | -1 | 9.44 | H | L | - | L | - |
| BGX001D | 214.7 | 234.7 | 0.86 | 1.65 | -1 | 10.45 | H | L | - | H | - |

| (1) Well ID | (2) z bot (ft) | (3) z top (ft) | (4) %sand | (5) slug Kh (ft/d) | (6) pump Kh (ft/d) | (7) modl Kh (ft/d) | (8) sand trend | (9) slug trend | (10) pump trend | (11) model trend | (12) Agree/ Dis- agree |
|----------------|----------------------|----------------------|--------------|-----------------------------|-----------------------------|-----------------------------|----------------------|----------------------|-----------------------|------------------------|---------------------------------|
| BGX002B | 137.2 | 147.2 | 0.72 | 0.21 | -1 | 5.64 | L | L | - | L | A |
| BGX002D | 181.1 | 191.1 | 0.86 | 0.34 | -1 | 9.14 | H | L | - | L | - |
| BGX003D | 201.6 | 221.6 | -1 | 1.85 | -1 | 11.21 | - | L | - | H | D |
| BGX004A | 106.8 | 116.8 | 0.92 | 1.83 | -1 | 12.66 | H | L | - | H | - |
| BGX004C | 170.7 | 180.7 | 0.87 | 1.16 | -1 | 12.16 | H | L | - | H | - |
| BGX004D | 203.8 | 223.8 | 0.66 | 2.89 | -1 | 1.01 | L | L | - | L | A |
| BGX005D | 195 | 215 | -1 | 1.45 | -1 | 10.76 | - | L | - | H | D |
| BGX006D | 191 | 211 | -1 | 3.57 | -1 | 14.2 | - | L | - | H | D |
| BGX007D | 194.1 | 214.1 | 0.9 | 20.4 | -1 | 18.68 | H | H | - | H | A |
| BGX009D | 212.4 | 232.4 | 0.88 | 0.36 | -1 | 10.51 | H | L | - | H | - |
| BGX010D | 216.2 | 236.2 | -1 | 0.52 | -1 | 8.44 | - | L | - | L | A |
| BGX012C | 174.1 | 184.1 | -1 | 1.11 | -1 | 8.96 | - | L | - | L | A |
| BGX012D | 223.7 | 243.7 | -1 | 0.36 | -1 | 7.83 | - | L | - | L | A |
| FC001A | 96.7 | 101.7 | -1 | 1.47 | -1 | 10.39 | - | L | - | H | D |
| FC001B | 151.8 | 156.8 | -1 | 0.07 | 0.05 | 1.3 | - | L | L | L | A |
| FC001C | 183.9 | 188.9 | -1 | 0 | -1 | 1.7 | - | L | - | L | A |
| FC002A | 53.1 | 57.1 | -1 | 8.39 | 1.2 | 5.23 | - | H | L | L | A |
| FC002B | 78.8 | 83.8 | -1 | 0.59 | 0.12 | 5.23 | - | L | L | L | A |
| FC002D | 159.2 | 164.2 | -1 | 2.73 | -1 | 11.82 | - | L | - | H | D |
| FC002E | 188.9 | 193.9 | -1 | 6.01 | -1 | 13.41 | - | H | - | H | A |
| FC002F | 207.3 | 212.3 | -1 | 1.9 | -1 | 3.17 | - | L | - | L | A |
| FC003B | 61.2 | 66.2 | -1 | 11.9 | -1 | 22.03 | - | H | - | H | A |
| FC003C | 121 | 126 | -1 | 1.66 | -1 | 11.09 | - | L | - | H | D |
| FC003D | 165.9 | 170.9 | -1 | 0.15 | -1 | 4.92 | - | L | - | L | A |
| FC003E | 185.7 | 190.7 | -1 | 1.39 | -1 | 10.63 | - | L | - | H | D |
| FC004B | 76.1 | 81.1 | -1 | 8.03 | -1 | 10.44 | - | H | - | H | A |
| FC004E | 176.4 | 181.4 | -1 | 4.79 | -1 | 16.21 | - | H | - | H | A |
| FC005B | 34.6 | 39.6 | -1 | 0.04 | -1 | 11 | - | L | - | H | D |
| FC005C | 70 | 75 | -1 | 0 | -1 | 11 | - | L | - | H | D |
| FC005D | 136.4 | 141.4 | -1 | 13 | -1 | 0.55 | - | H | - | L | D |
| FSB088C | 158.4 | 168.4 | -1 | 4.5 | -1 | 10.78 | - | H | - | H | A |
| FSB088D | 202.1 | 222.1 | -1 | 0.65 | -1 | 9.19 | - | L | - | L | A |
| FSB089C | 156.1 | 166.1 | 0.87 | 0.52 | -1 | 10.78 | H | L | - | H | - |
| FSB089D | 201.9 | 221.9 | 0.8 | 2.92 | -1 | 9.19 | H | L | - | L | - |
| FSB090C | 158.1 | 168.1 | -1 | 1.08 | -1 | 9.59 | - | L | - | L | A |

| (1) Well ID | (2) z bot (ft) | (3) z top (ft) | (4) %sand | (5) slug Kh (ft/d) | (6) pump Kh (ft/d) | (7) modl Kh (ft/d) | (8) sand trend | (9) slug trend | (10) pump trend | (11) model trend | (12) Agree/ Dis- agree |
|----------------|----------------------|----------------------|--------------|-----------------------------|-----------------------------|-----------------------------|----------------------|----------------------|-----------------------|------------------------|---------------------------------|
| FSB090D | 205.1 | 225.1 | -1 | 0.34 | -1 | 12.94 | - | L | - | H | D |
| FSB091C | 149.1 | 159.1 | 0.83 | 0.14 | -1 | 11.16 | H | L | - | H | - |
| FSB091D | 200.9 | 220.9 | 0.85 | 3.82 | -1 | 15.41 | H | L | - | H | - |
| FSB092C | 147.6 | 157.6 | -1 | 0.5 | -1 | 9.19 | - | L | - | L | A |
| FSB092D | 201.7 | 221.7 | -1 | 3.57 | -1 | 8.5 | - | L | - | L | A |
| FSB093C | 142 | 152 | 0.87 | 5.27 | -1 | 6.92 | H | H | - | L | D |
| FSB093D | 197.9 | 217.9 | 0.79 | 2.32 | -1 | 7.39 | H | L | - | L | - |
| FSB097A | 85.8 | 95.8 | 0.91 | 0.85 | -1 | 11.42 | H | L | - | H | - |
| FSB097C | 143.8 | 153.8 | 0.46 | 0.26 | -1 | 6.25 | L | L | - | L | A |
| FSB097D | 196.9 | 216.9 | 0.71 | 0.08 | -1 | 5.68 | L | L | - | L | A |
| FSB098C | 148.4 | 158.4 | 0.95 | 1.55 | -1 | 9.09 | H | L | - | L | - |
| FSB098D | 200.3 | 220.3 | 0.89 | 0.05 | -1 | 5.75 | H | L | - | L | - |
| FSB099C | 157.2 | 167.2 | 0.79 | 3.03 | -1 | 9.19 | H | L | - | L | - |
| FSB099D | 198.1 | 218.1 | 0.76 | 2.38 | -1 | 9.41 | L | L | - | L | A |
| FSB100A | 95.8 | 105.8 | 0.95 | 0.37 | -1 | 11.02 | H | L | - | H | - |
| FSB101A | 92.9 | 102.9 | 0.93 | 0.33 | -1 | 11.38 | H | L | - | H | - |
| FSB102C | 145.9 | 155.9 | -1 | 5.51 | -1 | 16.13 | - | H | - | H | A |
| FSB103C | 147.1 | 157.1 | -1 | 0.39 | -1 | 3.57 | - | L | - | L | A |
| FSB104C | 150.7 | 160.7 | -1 | 1.67 | -1 | 5.59 | - | L | - | L | A |
| FSB104D | 190.4 | 210.4 | -1 | 23.1 | -1 | 22.32 | - | H | - | H | A |
| FSB105C | 141.5 | 151.5 | -1 | 3.84 | -1 | 6.63 | - | L | - | L | A |
| FSB105D | 203.7 | 223.7 | -1 | 0.62 | -1 | 5.91 | - | L | - | L | A |
| FSB106C | 156 | 166 | -1 | 24 | -1 | 9.71 | - | H | - | L | D |
| FSB107C | 150.8 | 160.8 | -1 | 0.89 | -1 | 11.6 | - | L | - | H | D |
| FSB107D | 200.9 | 220.9 | -1 | 1.38 | -1 | 16.2 | - | L | - | H | D |
| FSB108D | 203.8 | 223.8 | -1 | 0.48 | -1 | 11.27 | - | L | - | H | D |
| FSB110D | 191.1 | 211.1 | -1 | 2.3 | -1 | 10.8 | - | L | - | H | D |
| FSB111C | 159 | 169 | -1 | 10.4 | 5.39 | 14.34 | - | H | L | H | D |
| FSB111D | 201.7 | 221.7 | -1 | 1.25 | -1 | 9.81 | - | L | - | L | A |
| FSB112A | 81 | 91 | 0.84 | 1.7 | -1 | 11.29 | H | L | - | H | - |
| FSB112C | 129.1 | 139.1 | 0.63 | 0.16 | -1 | 4.73 | L | L | - | L | A |
| FSB112D | 188.9 | 208.9 | 0.86 | 4.8 | -1 | 14.74 | H | H | - | H | A |
| FSB113A | 81 | 91.3 | 0.9 | 0.62 | -1 | 10.22 | H | L | - | H | - |
| FSB113C | 154 | 164 | 0.85 | 0.16 | -1 | 10.27 | H | L | - | H | - |
| FSB113D | 189.6 | 209.6 | 0.85 | 5.1 | -1 | 13.36 | H | H | - | H | A |

| (1) Well ID | (2) z bot (ft) | (3) z top (ft) | (4) %sand | (5) slug Kh (ft/d) | (6) pump Kh (ft/d) | (7) modl Kh (ft/d) | (8) sand trend | (9) slug trend | (10) pump trend | (11) model trend | (12) Agree/ Dis- agree |
|----------------|----------------------|----------------------|--------------|-----------------------------|-----------------------------|-----------------------------|----------------------|----------------------|-----------------------|------------------------|---------------------------------|
| FSB114A | 95.2 | 105 | 0.9 | 0.44 | -1 | 2.57 | H | L | - | L | - |
| FSB114C | 158 | 168 | 0.94 | 0.42 | -1 | 12.89 | H | L | - | H | - |
| FSB114D | 197.7 | 217.8 | 0.88 | 3.5 | -1 | 10.19 | H | L | - | H | - |
| FSB115C | 163.8 | 173.8 | 0.89 | 0.36 | -1 | 6.17 | H | L | - | L | - |
| FSB115D | 182.5 | 192.5 | 0.89 | 3.8 | -1 | 13.95 | H | L | - | H | - |
| FSB116C | 160.5 | 170.5 | 0.81 | 0.69 | -1 | 8.47 | H | L | - | L | - |
| FSB116D | 186.4 | 196.4 | 0.88 | 1.1 | -1 | 10.85 | H | L | - | H | - |
| FSB117D | 189.7 | 209.7 | -1 | 2.5 | -1 | 13.6 | - | L | - | H | D |
| FSB118D | 191.3 | 211.3 | -1 | 1.1 | -1 | 12.21 | - | L | - | H | D |
| FSB119D | 193.1 | 213.1 | -1 | 0.6 | -1 | 9.2 | - | L | - | L | A |
| FSB120A | 99 | 109 | 0.92 | 0.65 | -1 | 6.92 | H | L | - | L | - |
| FSB120C | 150.7 | 160.7 | 0.89 | 1.7 | -1 | 9.29 | H | L | - | L | - |
| FSB120D | 196.5 | 216.5 | 0.88 | 3.4 | -1 | 10.11 | H | L | - | H | - |
| FSB121C | 148.4 | 158.4 | 0.9 | 11 | -1 | 17.44 | H | H | - | H | A |
| FSB121DR | 191.3 | 211.3 | 0.89 | 0.27 | -1 | 10.03 | H | L | - | H | - |
| FSB122C | 160 | 170 | 0.85 | 2.6 | -1 | 13.6 | H | L | - | H | - |
| FSB122D | 186.6 | 206.6 | 0.88 | 1.6 | -1 | 12.42 | H | L | - | H | - |
| FSB123C | 155.3 | 165.3 | 0.93 | 6.7 | -1 | 13.88 | H | H | - | H | A |
| FSB123D | 194.1 | 214.1 | 0.93 | 3.9 | -1 | 15.23 | H | L | - | H | - |
| FSL001D | 208.5 | 228.6 | -1 | 0.58 | -1 | 6.66 | - | L | - | L | A |
| FSL002D | 208.7 | 228.8 | -1 | 0.25 | -1 | 6.37 | - | L | - | L | A |
| FSL003D | 205.9 | 226 | -1 | 0.88 | -1 | 8.96 | - | L | - | L | A |
| FSL004D | 204 | 224.1 | -1 | 0.79 | -1 | 9.72 | - | L | - | L | A |
| FSL005D | 203.5 | 223.7 | -1 | 3.02 | -1 | 9.95 | - | L | - | L | A |
| FSL006D | 202.1 | 222.1 | -1 | 0.89 | -1 | 10.3 | - | L | - | H | D |
| FSL007D | 199.5 | 219.6 | -1 | 0.59 | -1 | 10.55 | - | L | - | H | D |
| FSL008D | 202.7 | 222.8 | -1 | 0.41 | -1 | 8.53 | - | L | - | L | A |
| FSL009D | 201.4 | 221.5 | -1 | 0.56 | -1 | 8.99 | - | L | - | L | A |
| HAA001A | 94.9 | 104.9 | 0.93 | 5.34 | -1 | 0 | H | H | - | L | D |
| HAA001AA | 13.6 | 23.6 | 0.43 | 9.89 | -1 | 16.85 | L | H | - | H | - |
| HAA001B | 119.3 | 129.3 | 0.9 | 0.75 | -1 | 9.53 | H | L | - | L | - |
| HAA001C | 147.4 | 157.4 | 0.87 | 0.57 | -1 | 6.34 | H | L | - | L | - |
| HAA001D | 261.8 | 281.8 | 0.44 | 1.35 | -1 | 2.24 | L | L | - | L | A |
| HAA002AA | 29.4 | 39.4 | 0.89 | 25.25 | -1 | 22.33 | H | H | - | H | A |
| HAA002D | 260.3 | 280.4 | 0.51 | 0.01 | -1 | 1.18 | L | L | - | L | A |

| (1) Well ID | (2) z bot (ft) | (3) z top (ft) | (4) %sand | (5) slug Kh (ft/d) | (6) pump Kh (ft/d) | (7) modl Kh (ft/d) | (8) sand trend | (9) slug trend | (10) pump trend | (11) model trend | (12) Agree/ Dis- agree |
|----------------|----------------------|----------------------|--------------|-----------------------------|-----------------------------|-----------------------------|----------------------|----------------------|-----------------------|------------------------|---------------------------------|
| HAA003A | 96.8 | 106.8 | 0.91 | 0.64 | -1 | 10.19 | H | L | - | H | - |
| HAA003AA | 6.5 | 16.5 | 0.66 | 0.41 | -1 | 8.12 | L | L | - | L | A |
| HAA003B | 125.9 | 135.9 | 0.81 | 0.33 | -1 | 6.87 | H | L | - | L | - |
| HAA003C | 163.3 | 173.3 | 0.85 | 0.13 | -1 | 5.17 | H | L | - | L | - |
| HAA005A | 100.7 | 110.7 | -1 | 8.69 | -1 | 0 | - | H | - | L | D |
| HAA005C | 177.7 | 187.7 | -1 | 3.3 | -1 | 8.11 | - | L | - | L | A |
| HAA006A | 95.6 | 105.6 | 0.99 | 1.41 | -1 | 13.6 | H | L | - | H | - |
| HAA006AA | 25.8 | 35.8 | 0.89 | 0.24 | -1 | 8.07 | H | L | - | L | - |
| HAA006B | 131.3 | 141.4 | 0.81 | 0.08 | -1 | 4.46 | H | L | - | L | - |
| HAA006C | 161.1 | 171.1 | 0.9 | 23 | -1 | 19.12 | H | H | - | H | A |
| HAA006D | 247.1 | 267.2 | 0.77 | 1.29 | -1 | 7.8 | L | L | - | L | A |
| HC001A | 89.5 | 94.5 | 0.92 | 0.56 | -1 | 14 | H | L | - | H | - |
| HC001B | 133.5 | 138.5 | -1 | 1.28 | -1 | 0.92 | - | L | - | L | A |
| HC001C | 183.5 | 188.5 | -1 | 4.28 | 0.95 | 0.96 | - | H | L | L | A |
| HC001D | 206.5 | 211.5 | -1 | 1.17 | -1 | 9.49 | - | L | - | L | A |
| HC001E | 251.5 | 256.5 | -1 | 12.3 | -1 | 12.44 | - | H | - | H | A |
| HC002A | 72.2 | 77.2 | 0.91 | 2.83 | -1 | 13.96 | H | L | - | H | - |
| HC002B | 85.7 | 90.7 | -1 | 1.17 | -1 | 14 | - | L | - | H | D |
| HC002C | 135.7 | 140.7 | -1 | 0.34 | -1 | 0.91 | - | L | - | L | A |
| HC002D | 178.2 | 183.2 | -1 | 3.59 | -1 | 0.96 | - | L | - | L | A |
| HC002E | 205.7 | 210.7 | -1 | 2.16 | 0.62 | 8.16 | - | L | L | L | A |
| HC002F | 250.7 | 255.7 | -1 | 12.3 | 1.8 | 12.44 | - | H | L | H | D |
| HC002H | 154.7 | 164.7 | -1 | 0.85 | -1 | 0.92 | - | L | - | L | A |
| HC003A | 65.6 | 70.6 | 0.91 | 12.5 | 2.6 | 15.41 | H | H | L | H | - |
| HC003B | 104.1 | 109.1 | -1 | 12 | -1 | 5.17 | - | H | - | L | D |
| HC003E | 202.1 | 207.1 | -1 | 2.45 | -1 | 8.98 | - | L | - | L | A |
| HC003F | 240.6 | 245.6 | -1 | 14.6 | -1 | 14.61 | - | H | - | H | A |
| HC004A | 150 | 155 | 0.78 | 1.54 | 0.35 | 8.09 | H | L | L | L | A |
| HC004B | 200 | 205 | -1 | 1.01 | 0.23 | 7.76 | - | L | L | L | A |
| HC005A | 156.5 | 161.5 | 0.82 | 0.42 | -1 | 8.87 | H | L | - | L | - |
| HC005B | 198 | 203 | -1 | 4.73 | -1 | 10.62 | - | H | - | H | A |
| HC006A | 156.2 | 161.2 | 0.88 | 1.55 | 0.24 | 3.45 | H | L | L | L | A |
| HC006B | 210.2 | 215.2 | -1 | 2.17 | 0.42 | 7.34 | - | L | L | L | A |
| HC008B | 132.5 | 137.5 | -1 | 5.99 | 1.2 | 12.3 | - | H | L | H | D |
| HC008C | 187.3 | 192.3 | -1 | 4.73 | 0.5 | 10.03 | - | H | L | H | D |

| (1) Well ID | (2) z bot (ft) | (3) z top (ft) | (4) %sand | (5) slug Kh (ft/d) | (6) pump Kh (ft/d) | (7) modl Kh (ft/d) | (8) sand trend | (9) slug trend | (10) pump trend | (11) model trend | (12) Agree/ Dis- agree |
|----------------|----------------------|----------------------|--------------|-----------------------------|-----------------------------|-----------------------------|----------------------|----------------------|-----------------------|------------------------|---------------------------------|
| HC010B | 164.8 | 169.8 | -1 | 0.91 | -1 | 11.04 | - | L | - | H | D |
| HC011C | 190.8 | 195.8 | -1 | 1.01 | -1 | 8.82 | - | L | - | L | A |
| HC012B | 177.3 | 182.3 | -1 | 5.09 | -1 | 11.36 | - | H | - | H | A |
| HC013B | 193.3 | 198.3 | -1 | 0.45 | 0.09 | 3.05 | - | L | L | L | A |
| HC015B | 163 | 168 | -1 | 4.09 | -1 | 15.78 | - | L | - | H | D |
| HC035D | 87.8 | 92.8 | 0.89 | 0.19 | -1 | 11.46 | H | L | - | H | - |
| HCA004A | 103.7 | 113.7 | 0.91 | 8.53 | -1 | 1.57 | H | H | - | L | D |
| HCA004AA | 33.6 | 43.6 | 0.97 | 13.9 | -1 | 25.44 | H | H | - | H | A |
| HCA004B | 126.6 | 136.6 | 0.81 | 0.19 | -1 | 5.56 | H | L | - | L | - |
| HCA004C | 153.8 | 163.8 | 0.92 | 1.59 | -1 | 11.86 | H | L | - | H | - |
| HMD002D | 190.8 | 210.8 | 0.89 | 4.14 | -1 | 12.96 | H | H | - | H | A |
| HMD003D | 187.7 | 207.7 | 0.91 | 0.26 | -1 | 10.66 | H | L | - | H | - |
| HSB069A | 83.1 | 93.1 | 0.93 | 8.79 | -1 | 21.75 | H | H | - | H | A |
| HSB070C | 164.9 | 174.9 | -1 | 0.25 | -1 | 5.27 | - | L | - | L | A |
| HSB071C | 171.9 | 181.9 | -1 | 0.22 | -1 | 4.91 | - | L | - | L | A |
| HSB100C | 153 | 163 | -1 | 1.39 | -1 | 10.55 | - | L | - | H | D |
| HSB100D | 216.9 | 236.9 | -1 | 1.77 | -1 | 10.45 | - | L | - | H | D |
| HSB101C | 166.3 | 176.3 | 0.81 | 4 | 1.68 | 10.44 | H | L | L | H | D |
| HSB101D | 216.1 | 236.1 | 0.73 | 2.7 | -1 | 8.8 | L | L | - | L | A |
| HSB102C | 166.7 | 176.7 | -1 | 2 | -1 | 7.37 | - | L | - | L | A |
| HSB102D | 216.3 | 236.3 | -1 | 0.31 | -1 | 10.52 | - | L | - | H | D |
| HSB103C | 159.2 | 169.2 | 0.76 | 3.15 | -1 | 10.39 | L | L | - | H | D |
| HSB103D | 213.7 | 233.7 | 0.81 | 3.02 | -1 | 17.61 | H | L | - | H | - |
| HSB104C | 163.5 | 173.5 | -1 | 0.64 | -1 | 5.83 | - | L | - | L | A |
| HSB104D | 210.6 | 230.6 | -1 | 24.65 | -1 | 13.58 | - | H | - | H | A |
| HSB105C | 152.2 | 162.2 | 0.86 | 4.28 | -1 | 10.84 | H | H | - | H | A |
| HSB105D | 211.8 | 231.8 | 0.57 | 36.15 | -1 | 8.84 | L | H | - | L | - |
| HSB106C | 158.7 | 168.7 | -1 | 24.4 | -1 | 12.61 | - | H | - | H | A |
| HSB106D | 210.7 | 230.7 | -1 | 13.2 | -1 | 18.52 | - | H | - | H | A |
| HSB107C | 159.3 | 169.3 | 0.9 | 0.98 | -1 | 11.24 | H | L | - | H | - |
| HSB107D | 215.1 | 235.1 | 0.5 | 9.28 | -1 | 17.53 | L | H | - | H | - |
| HSB108C | 186 | 196 | -1 | 0.98 | -1 | 0.12 | - | L | - | L | A |
| HSB108D | 212 | 232 | -1 | 7.28 | -1 | 16.29 | - | H | - | H | A |
| HSB109C | 168.4 | 178.4 | 0.82 | 0.95 | -1 | 7.53 | H | L | - | L | - |
| HSB109D | 213 | 233 | 0.81 | 5.23 | -1 | 10.77 | H | H | - | H | A |

| (1) Well ID | (2) z bot (ft) | (3) z top (ft) | (4) %sand | (5) slug Kh (ft/d) | (6) pump Kh (ft/d) | (7) modl Kh (ft/d) | (8) sand trend | (9) slug trend | (10) pump trend | (11) model trend | (12) Agree/ Dis- agree |
|----------------|----------------------|----------------------|--------------|-----------------------------|-----------------------------|-----------------------------|----------------------|----------------------|-----------------------|------------------------|---------------------------------|
| HSB110C | 171.4 | 181.4 | -1 | 0.71 | -1 | 6.64 | - | L | - | L | A |
| HSB110D | 211.4 | 231.4 | -1 | 23.87 | -1 | 13.96 | - | H | - | H | A |
| HSB111C | 140.7 | 150.7 | 0.73 | 1.65 | -1 | 11.7 | L | L | - | H | D |
| HSB111E | 211.7 | 231.7 | 0.89 | 38.2 | -1 | 8.64 | H | H | - | L | D |
| HSB112C | 140.6 | 150.6 | -1 | 4.17 | -1 | 10.57 | - | H | - | H | A |
| HSB113C | 151.7 | 161.7 | 0.84 | 0.99 | -1 | 9.4 | H | L | - | L | - |
| HSB113D | 216.2 | 236.2 | 0.65 | 4.73 | -1 | 13.53 | L | H | - | H | - |
| HSB114C | 185.6 | 195.6 | -1 | 2.86 | -1 | 10.38 | - | L | - | H | D |
| HSB114D | 212.8 | 232.8 | -1 | 3.46 | -1 | 13.71 | - | L | - | H | D |
| HSB115C | 182.8 | 192.8 | 0.84 | 0.46 | -1 | 1.15 | H | L | - | L | - |
| HSB115D | 213.9 | 233.9 | 0.74 | 1.47 | -1 | 10.19 | L | L | - | H | D |
| HSB116C | 180.5 | 190.5 | -1 | 4.36 | -1 | 7 | - | H | - | L | D |
| HSB116D | 214.5 | 234.5 | -1 | 1.71 | -1 | 8.53 | - | L | - | L | A |
| HSB117A | 84.8 | 94.8 | 0.91 | 0.16 | -1 | 10.18 | H | L | - | H | - |
| HSB117C | 165.1 | 175.1 | 0.88 | 0.57 | -1 | 9.68 | H | L | - | L | - |
| HSB117D | 200.3 | 220.3 | 0.71 | 7.2 | -1 | 15.35 | L | H | - | H | - |
| HSB118A | 91 | 101 | 0.86 | 12 | -1 | 12.6 | H | H | - | H | A |
| HSB122A | 85.4 | 95.4 | 0.86 | 6.8 | -1 | 14.11 | H | H | - | H | A |
| HSB125C | 145.6 | 155.6 | -1 | 0.86 | -1 | 9.65 | - | L | - | L | A |
| HSB125D | 199.4 | 219.4 | -1 | 5.67 | -1 | 14.69 | - | H | - | H | A |
| HSB126C | 176.3 | 181.3 | -1 | 56.7 | -1 | 4.46 | - | H | - | L | D |
| HSB126D | 190.5 | 200.5 | -1 | 1.29 | -1 | 10.35 | - | L | - | H | D |
| HSB127C | 148.4 | 158.4 | -1 | 0.82 | -1 | 14.16 | - | L | - | H | D |
| HSB127D | 197.8 | 217.8 | -1 | 13.63 | -1 | 17.44 | - | H | - | H | A |
| HSB129C | 147.8 | 157.8 | -1 | 0.55 | -1 | 7.89 | - | L | - | L | A |
| HSB129D | 185.2 | 205.2 | -1 | 2.78 | -1 | 14.49 | - | L | - | H | D |
| HSB130C | 159.9 | 169.9 | -1 | 70.85 | 94.5 | 59.89 | - | H | H | H | A |
| HSB130D | 182.1 | 202.1 | -1 | 0.45 | 0.26 | 4.84 | - | L | L | L | A |
| HSB131C | 148.5 | 158.5 | -1 | 136 | -1 | 32.47 | - | H | - | H | A |
| HSB131D | 195.7 | 205.7 | -1 | 6.77 | 65.96 | 21.26 | - | H | H | H | A |
| HSB132C | 168.6 | 178.6 | -1 | 0.28 | -1 | 4.99 | - | L | - | L | A |
| HSB132D | 206.5 | 226.5 | -1 | 6.3 | -1 | 15.17 | - | H | - | H | A |
| HSB133D | 208.5 | 228.5 | -1 | 0.08 | -1 | 8.66 | - | L | - | L | A |
| HSB134C | 149.1 | 159.1 | -1 | 1.31 | -1 | 10.74 | - | L | - | H | D |
| HSB134D | 205.8 | 225.8 | -1 | 7.01 | -1 | 19.06 | - | H | - | H | A |

| (1) Well ID | (2) z bot (ft) | (3) z top (ft) | (4) %sand | (5) slug Kh (ft/d) | (6) pump Kh (ft/d) | (7) modl Kh (ft/d) | (8) sand trend | (9) slug trend | (10) pump trend | (11) model trend | (12) Agree/ Dis- agree |
|----------------|----------------------|----------------------|--------------|-----------------------------|-----------------------------|-----------------------------|----------------------|----------------------|-----------------------|------------------------|---------------------------------|
| HSB135C | 147.3 | 157.3 | -1 | 20.01 | -1 | 14.56 | - | H | - | H | A |
| HSB136C | 160.5 | 170.5 | -1 | 0.61 | -1 | 4.48 | - | L | - | L | A |
| HSB136D | 200.2 | 220.2 | -1 | 9.05 | -1 | 17.19 | - | H | - | H | A |
| HSB137D | 205.3 | 225.3 | -1 | 2.07 | -1 | 11.8 | - | L | - | H | D |
| HSB139A | 87.6 | 97.6 | 0.86 | 3.82 | -1 | 13.12 | H | L | - | H | - |
| HSB139D | 206.7 | 226.7 | 0.74 | 6.52 | -1 | 15.21 | L | H | - | H | - |
| HSB140A | 81 | 91 | 0.9 | 12 | -1 | 18.2 | H | H | - | H | A |
| HSB140C | 161.6 | 171.6 | 0.9 | 0.61 | -1 | 9.01 | H | L | - | L | - |
| HSB140D | 194.1 | 214.1 | 0.79 | 4 | -1 | 12.8 | H | L | - | H | - |
| HSB141A | 80.6 | 90.6 | 0.94 | 1.9 | -1 | 13.98 | H | L | - | H | - |
| HSB141C | 154.7 | 164.7 | 0.86 | 9 | -1 | 13.82 | H | H | - | H | A |
| HSB141D | 217.8 | 237.8 | 0.72 | 0.59 | -1 | 8.75 | L | L | - | L | A |
| HSB142C | 161.6 | 171.6 | 0.9 | 0.6 | -1 | 10.22 | H | L | - | H | - |
| HSB142D | 189.7 | 199.7 | 0.62 | 0.68 | -1 | 0.49 | L | L | - | L | A |
| HSB143C | 169.1 | 179.1 | 0.93 | 2.4 | -1 | 14.1 | H | L | - | H | - |
| HSB143D | 196.9 | 216.9 | 0.75 | 9.5 | -1 | 12.42 | L | H | - | H | - |
| HSB144A | 78.6 | 88.6 | 0.95 | 0.22 | -1 | 15.57 | H | L | - | H | - |
| HSB145C | 164.7 | 174.7 | 0.8 | 0.38 | -1 | 6.67 | H | L | - | L | - |
| HSB145D | 184.2 | 194.2 | 0.88 | 0.33 | -1 | 7.02 | H | L | - | L | - |
| HSB146A | 85.5 | 95.5 | 0.87 | 9.4 | -1 | 16.44 | H | H | - | H | A |
| HSB146C | 152.3 | 162.3 | 0.76 | 0.68 | -1 | 7.38 | L | L | - | L | A |
| HSB146D | 204 | 224.1 | 0.71 | 1.6 | -1 | 8.1 | L | L | - | L | A |
| HSB147D | 215.2 | 235.2 | -1 | 0.67 | -1 | 7.77 | - | L | - | L | A |
| HSB148C | 158.9 | 168.9 | 0.78 | 1.8 | -1 | 10.4 | H | L | - | H | - |
| HSB148D | 198.1 | 218.1 | 0.87 | 0.42 | -1 | 9.13 | H | L | - | L | - |
| HSB149D | 207 | 227 | -1 | 2.9 | -1 | 13.21 | - | L | - | H | D |
| HSB150D | 206.9 | 226.9 | -1 | 1.2 | -1 | 13.24 | - | L | - | H | D |
| HSB151C | 170.6 | 180.6 | 0.88 | 0.8 | -1 | 10 | H | L | - | L | - |
| HSB151D | 197.6 | 207.6 | 0.8 | 2.3 | -1 | 11.65 | H | L | - | H | - |
| HSB152C | 173.1 | 183.1 | 0.8 | 0.8 | -1 | 7.25 | H | L | - | L | - |
| HSB152D | 197 | 207 | 0.87 | 1.1 | -1 | 10.57 | H | L | - | H | - |
| HSL001D | 219.8 | 239.8 | -1 | 5.51 | -1 | 9.22 | - | H | - | L | D |
| HSL002D | 225.2 | 245.3 | -1 | 1.44 | -1 | 18.88 | - | L | - | H | D |
| HSL003D | 233.7 | 253.8 | -1 | 0.52 | -1 | 10.13 | - | L | - | H | D |
| HSL004D | 245 | 265.1 | -1 | 1.19 | -1 | 8.52 | - | L | - | L | A |

| (1) Well ID | (2) z bot (ft) | (3) z top (ft) | (4) %sand | (5) slug Kh (ft/d) | (6) pump Kh (ft/d) | (7) modl Kh (ft/d) | (8) sand trend | (9) slug trend | (10) pump trend | (11) model trend | (12) <u>A</u> gree/ <u>D</u> is- <u>a</u> gree |
|----------------|----------------------|----------------------|--------------|-----------------------------|-----------------------------|-----------------------------|----------------------|----------------------|-----------------------|------------------------|---|
| HSL005D | 247.8 | 267.7 | -1 | 0.9 | -1 | 10.61 | - | L | - | H | D |
| HSL006A | 104.7 | 114.7 | 0.92 | 5.76 | -1 | 0.1 | H | H | - | L | D |
| HSL006AA | 18.6 | 28.6 | 0.91 | 5.49 | -1 | 15.19 | H | H | - | H | A |
| HSL006B | 127.9 | 137.9 | 0.87 | 0.2 | -1 | 9.33 | H | L | - | L | - |
| HSL006C | 157.6 | 167.6 | 0.82 | 4.65 | -1 | 8.37 | H | H | - | L | D |
| HSL006D | 243.9 | 264 | 0.76 | 1.32 | -1 | 9.93 | L | L | - | L | A |
| HSL007D | 242.3 | 262.4 | -1 | 1.84 | -1 | 9.93 | - | L | - | L | A |
| HSL008D | 248.4 | 268.4 | 0.45 | 1.93 | -1 | 4.8 | L | L | - | L | A |
| M037A | 225 | 227 | -1 | 0.24 | -1 | 7.4 | - | L | - | L | A |
| SDS003A | 210.5 | 230.5 | -1 | 2.75 | -1 | 12.69 | - | L | - | H | D |
| SDS004 | 185.4 | 205.4 | -1 | 3.87 | -1 | 12.96 | - | L | - | H | D |
| SDS007A | 75 | 80 | -1 | 0.06 | -1 | 16.96 | - | L | - | H | D |
| SDS012A | 136.4 | 141.4 | 0.92 | 1.21 | -1 | 1.79 | H | L | - | L | - |
| SDS012B | 186.7 | 191.7 | 0.88 | 0.08 | -1 | 7.02 | H | L | - | L | - |
| SDS017 | 196.6 | 216.6 | -1 | 3.31 | -1 | 11.4 | - | L | - | H | D |
| YSC001C | 197.5 | 207.5 | 0.91 | 2.4 | -1 | 12.4 | H | L | - | H | - |
| YSC002D | 197.9 | 218 | 0.83 | 1.19 | -1 | 11.82 | H | L | - | H | - |
| YSC004C | 195.9 | 205.9 | 0.8 | 1.26 | -1 | 9.72 | H | L | - | L | - |
| YSC005A | 116 | 121 | 0.99 | 0.71 | -1 | 10.43 | H | L | - | H | - |

APPENDIX B – DESIGN CHECKING COMMENTS AND RESPONSES/RESOLUTIONS.

Design checking was performed by S. Aleman.

| Document Review Comments | | | | Page 1 of 5 | |
|------------------------------------|---------------------------------|--|--|---------------------|-----|
| Document No. WSRC-TR-2004-00106 | Rev. 0 | Title: Groundwater Flow Model of the General Separations Area Using PORFLOW (U) | Comments Due 04/23/2004 | Reviewer Concur | |
| # | Section/Page/ Paragraph/Line | Comment | Response/Resolution | Reviewer Initial | |
| 1 | Page iii | Add ACR and FACT to acronym list. "Limit" should be "Limited". "tank clay confining unit" should be "Tan Clay Confining Unit" | Agreed | | Yes |
| 2 | Page 1/P1 | State that PORFLOW utilizes control volume discretization | Agreed | | Yes |
| 3 | Page 1/P2/L1 | Eliminate "combined" and "contaminant transport" since you are only interested in translating the steady-state groundwater flow model from FACT. | Agreed; text reworded | | Yes |
| 4 | Page 1/P2 | Where is the procedure or algorithm for translating the Darcy velocity field from FACT to PORFLOW documented? | Process is undocumented. revised text states this fact. | | Yes |
| 5 | Page 1/P3 | Instead of using "drawback" I would just emphasize the differences between the element/cell numbering. | Agreed; "drawback" replaced with "issue" | | Yes |
| 6 | Page 1/P4 | Change "drawback" to "differences". Emphasize using the same code (PORFLOW) for both groundwater flow and transport simulations. | Agreed | | Yes |
| 7 | Page 1/P5 | The verification and validation testing should be addressed in the "Software Quality Assurance Plan for the PORFLOW code" for the version of the code you plan to use for PA work. | Text revised to tie V&V testing for PORFLOW version 5.95.0 documented in present report to the PORFLOW Software QA Plan | | Yes |
| 8 | Page 3/P2 | Highly distorted elements in FACT do not present a problem numerically for the influence matrix formulation or 2-point Gauss-Legendre quadrature. The Gaussian quadrature option provides a superior representation of the Darcian velocity field for highly distorted elements. | Text revised as suggested | | Yes |
| 9 | Page 3/P2 | You mentioned concern about low Courant numbers. Is there any concern about high cell Pedit numbers? | I don't think so. Smaller cells are beneficial. $Pe = \frac{v \Delta x}{D} < 2$ However, "low cell Courant" corrected to read "high cell Courant" number. $Co = \frac{v \Delta t}{\Delta x} < 1$ | | NC |
| 10 | Page 3/P6 | Section 2-5 should be Section 2.5 | Agreed | | Yes |
| 11 | Page 3/P7 | What was the rationale for applying both recharge/drain and GH boundary conditions at the same node in the GSA/FACT model? | Not sure. Possibly an oversight, or possibly done as a convenience (easy to specify recharge/drain over entire top surface) | | Yes |

| Document Review Comments | | | | | Page 2 of 5 |
|------------------------------------|---------------------------------|---|------------------|--|-----------------------------|
| Document No. WSRC-TR-2004-00106 | Rev 0 | Title: Groundwater Flow Model of the General Separations Area Using PORFLOW (U) | Reviewer Initial | Response/Resolution | Comments Due: 04/23/2004 |
| # | Section/Page/ Paragraph/Line | Comment | Reviewer Initial | Response/Resolution | Reviewer Concur |
| 12 | Page 4/Eq. 2-1 | Provide the reference for Eq. 2-1. | | No reference exists. The equation was invented to mitigate numerical convergence problems. "chosen" added to text for clarification | Yes |
| 13 | Page 4/P1 | Change section 2-4 to Section 2.4. | | Agreed | Yes |
| 14 | Page 4/P3 | Change section 2-5 to Section 2.5. | | Agreed | Yes |
| 15 | Page 4/P5 | Please clarify explanation on how prescribed head boundary conditions are applied in PORFLOW. | | Text rewritten to be more clear. | Yes |
| 16 | Page 4/P7 | Elaborate on how the recharge/drain or equivalent BC is implemented within the PORFLOW framework. | | Additional explanation provided in Section 2.4, now entitled "Implementation of Recharge/Drain BC" | Yes |
| 17 | Page 5/P1 | Change section 2-5 to Section 2.5. section 2-6 should be changed to Section 2.5. | | Agreed | Yes |
| 18 | Page 5/P3 | What is the justification for setting the horizontal and vertical conductivities in the vadose zone to 0.1 ft/d? Change "straight down" to "vertically downward". How does the homogeneous and isotropic nature of the K field ensure vertical moisture movement in the vadose zone? To ensure vertical moisture movement, the horizontal components of the hydraulic conductivity tensor (product of relative permeability and saturated conductivity) have to be set to zero in the vadose zone. How do you implement that in PORFLOW? The recharge/drain BC introduces numerical nonlinearity. Remove or rewrite sentence discussing numerical instability. | | Text rewritten to provide better explanation/justification. The horizontal components are not set to zero, because some horizontal movement is acceptable. | Yes |
| 19 | Page 5/P4 | The recharge/drain BC introduces numerical nonlinearity. Remove or rewrite sentence discussing numerical instability. | | Agreed | Yes |
| 20 | Page 5/P5 | Why did you not use a Cauchy (mixed) boundary condition to simulate the FACT recharge/drain BC? Can you show mathematically, how the calculation sequence given in Section 2.4 is equivalent to the recharge/drain BC. | | Cauchy/mixed BC providing recharge/drain functionality is not offered in PORFLOW. Equation (2-2) is the recharge/drain BC. The rest of the algorithm is a Picard iteration to ensure the boundary pressure is synchronized with the recharge/drain flux | Yes |
| 21 | Page 5 | Section 2.4 is not really dealing with numerical issues but a code deficiency in PORFLOW to emulate the recharge/drain BC. Perhaps you should try to get the code developers of PORFLOW to implement the recharge/drain BC. | | The section has been renamed to "Implementation of Recharge/Drain BC". Good suggestion | Yes |
| 22 | Page 6/S2.5/P1 | Remove "as high as" | | Agreed | Yes |

| Document Review Comments | | | Page 3 of 5 |
|------------------------------------|---------------------------------|--|---|
| Document No. WSRC-TR-2004-00106 | Rev. 0 | Title: Groundwater Flow Model of the General Separations Area Using PORFLOW (U) | Comments Due: 04/23/2004 |
| # | Section/Page/ Paragraph/Line | Comment | Response/Resolution |
| 23 | Page 6/S2.5/P2 | How much longer were the travel times computed by PORFLOW? What was the cause for the differences, other than recharge flux? | A quantitative comparison of travel times was not done - just visual. Differences in the vertical grids and conductivity fields apparently caused some difference in flow direction and speed. Also differences in spatial averaging/interpolation of the K field by the two codes had an impact. |
| 24 | Page 6/S2.5 | The changes in conductivity values relative to the GSA/FACT model for the three zones described seem pretty large. Is that an artifact of the geometric averaging of hydraulic conductivities used in PORFLOW. | Differences were larger than anticipated. Seems to be a result of the factors mentioned in #23 |
| 25 | Page 11 | In Figure 2-6 do you mean "horizontal" or "vertical"? | Horizontal as in Kh |
| 26 | Page 12 | In Figure 2-8 can you show a line that delineates the water table (red line)? | Water table marker added |
| 27 | Page 13/S3.1 | Add a Table 3-2 showing the summary statistics for the GSA/FACT model. | Provided in Table 4-4 |
| 28 | Page 13/S3.2 | In your discussion, groundwater discharge corresponds to negative fluxes. In Figure 3-7, groundwater discharge areas are indicated by positive values. | Text corrected |
| 29 | Page 14 | Add a column to Table 3-2 showing the simulated stream baseflows for the GSA/FACT model. | Provided in Table 4-5 |
| 30 | Page 15 | What is the significance of the model cross-section at I=50? | Caption revised to indicate slice through E Area |
| 31 | Page 19 | See Comment 28. | See Comment 28 |
| 32 | Page 20/S4.0 | Verification and Validation activities should be addressed in the Software Quality Assurance Plan. | Agreed. The V&V tests performed within this project are now related to the PORFLOW Software QA Plan |
| 33 | Page 20/S4.1 | Rename section to Global Mass Balance | Disagree. The section contains both global (Table 4-1) and cell-by-cell mass balances (Table 4-2) |
| 34 | Page 20/S4.1/P1 | Darcy's law is implicitly satisfied since it is substituted into the continuity equation. | At the theory level, agreed. The purpose of the test is to ensure that Richards equation has been correctly coded |
| 35 | Page 20/S4.1/P2 | Your statement about "the net volumetric flow entering the model grid should be zero" is only true if you do not have any internal sources or sinks. | Agreed. Text revised accordingly |
| 36 | Page 21/Table 4-2 | Replacing Table 4-2 with a table showing a detailed water budget would be more useful and informative. | Table 4-1 provides a water budget for the entire model domain. Table 4-2 confirms mass conservation on a cell-by-cell basis |

| Document Review Comments | | | | Page 4 of 5 |
|------------------------------------|---------------------------------|---|--|--------------------|
| Document No. WSRC-TR-2004-00106 | Rev. 0 | Title: Groundwater Flow Model of the General Separations Area Using PORFLOW (U) | Comments Due: 04/23/2004 | Reviewer Concur |
| # | Section/Page/ Paragraph/Line | Comment | Response/Resolution | Reviewer Concur |
| 37 | Page 21/S4.2 | Section 4.2 should be assessing particle tracking based on the Darcian velocity field generated by PORFLOW. As mentioned in Comment 34, Darcy's law is implicitly satisfied. The issue to address here is how accurately PORFLOW computes the Darcy velocities from the head solution for distorted and non-distorted meshes. Again, this should be addressed in the Software Quality Assurance Plan. | The purpose of the test is to ensure that Richards equation, which contains Darcy's Law, has been adequately implemented. The independent calculation assumes the mesh is mildly distorted as most. This assumption should be consistent with the GSA/PORFLOW mesh, which was designed to minimize mesh distortion | Yes |
| 38 | Page 22/S4.4 | Change section 5.5 to Section 5.5. | Agreed | Yes |
| 39 | Page 23/S4.5 | Table 4-4 should be complemented with a table showing the GSA/PORFLOW results. | Complementary information provided in Table 3-1 | Yes |
| 40 | Page 23/S4.6 | Table 4-5 should be complemented with a table showing the GSA/PORFLOW results. | Complementary information provided in Table 3-2 | Yes |
| 41 | Page 24/S4.7 | How was the solute transport model calibrated in the GSA/PORFLOW model? There is no mention about transport parameter settings (dispersivities, etc). Provide a more detailed discussion about solute transport calibration. | Some additional description of transport simulations provided | Yes |
| 42 | Page 24/S4.8 | Remove discussions on mass conservation and Darcy's law per previous comments. | Discussion now related to PORFLOW Software QA Plan | Yes |
| 43 | Page 29/S5.0 | A recommendation should be made to update the "Software Quality Assurance Plan for PORFLOW" prior to performing PA analyses. | The limited extent of software QA testing of PORFLOW version 5.95.0 is stated, and caution that additional testing would be required for other uses | Yes |
| 44 | Page A-1 | Fix table labels. Perhaps go to landscape mode. Set Table Heading Rows to repeat. | Agreed | Yes |
| 45 | General | Section 3 should discuss the steady-state groundwater flow simulations. Section 4 should be an assessment of particle tracking and solute transport. V&V should be addressed per Comment 7. | Addressed in other comments | Yes |

| Document Review Comments | | | | Page 5 of 5 |
|---|---|---|---------------------------------------|--------------------|
| Document No. WSRC-TR-2004-00106 | Rev 0 | Title: Groundwater Flow Model of the General Separations Area Using PORFLOW (U) | Comments Due: 04/23/2004 | Reviewer Concur |
| # | Section/Page/ Paragraph/Line | Comment | Response/Resolution | Reviewer Concur |
| Reviewer Name | Sebastian Aleman / SEA Print Name / Initials | Signature | Phone / Location: 5-8040 / 773-42A | Date 11-May-04 |
| Concurrence Signature QA Reviewer | _____ / _____ | _____ / _____ | Phone / Location: | Date |

Distribution

| | |
|---------------------|-----------------|
| Goldston, W.T. | 705-3C, Rm 105 |
| Flach, G. P. | 773-42A, Rm 211 |
| Harris, M. K. | 773-42A, Rm 219 |
| Aleman, S. E. | 773-42A, Rm 147 |
| Stevens, W. T. | 773-A, Rm A-261 |
| Butcher, B. T. | 773-43A, Rm 216 |
| Wilhite, E. L. | 773-43A, Rm 214 |
| Collard, L. B. | 773-43A, Rm 207 |
| Cook, J. R. | 773-43A, Rm 209 |
| Hiergesell, R. A. | 773-42A, Rm 251 |
| STI (3) | 703-43A |
| WPT File | 773-43A, Rm 213 |
| SW Document Control | 642-E |